Title: Medial entorhinal cortex plays a specialized role in learning of flexible, context-dependent interval timing behavior

Authors: Erin R. Bigus[1+], Hyun-Woo Lee[2+], Jiani Shi[2], James G. Heys[2*]

Affiliations:
[1] Interdepartmental PhD Program in Neuroscience, University of Utah
[2] Department of Neurobiology, University of Utah, Salt Lake City, UT 84112, USA

* correspondence to: jim.heys@neuro.utah.edu
+ indicates equal contribution

Abstract

In order to survive and adapt in a dynamic environment, animals must perceive and remember the temporal structure of events and actions across a wide range of timescales. Prior research to investigate the neurobiological basis underlying so-called interval timing (i.e. timing on the scale of second to minutes) has focused largely on simple timing tasks that require animals to discriminate and/or reproduce stimuli presented at single, fixed durations over thousands of trials. Perhaps not surprisingly, this work has uncovered circuits involved in procedural memory systems, such as the basal ganglia, that play a key role in learning and driving timing behavior. Episodic memory (i.e. the ability to remember specific, personal events that occur in spatial and temporal context) also requires accurate temporal processing and is known to require neural circuits in the medial temporal lobe (MTL), including entorhinal cortex. However, a clear role for medial temporal lobe structures in interval timing has been conspicuously lacking. In order to determine the specific role that MTL structures play in timing behavior, we developed a novel behavioral paradigm that requires learning complex temporal contingencies. Applying this novel interval timing task in mice, in concert with methods for manipulating neural activity and methods for large-scale cellular resolution neurophysiological recording, we have uncovered a specific role for medial entorhinal cortex (MEC) in flexible, context-dependent learning of interval timing behavior. We find neurons in MEC, termed time cells, fire in regular time-locked sequences during timing. Remarkably, over the course of learning, these neural dynamics become context-dependent with specific sub-populations of neurons becoming selectively active within particular trial contexts. We also find that this neural activity is disrupted when animals make errors in their timing behavior and that animals are completely unable to learn this timing behavior without MEC activity. Further, we find that MEC activity is not necessary for very rigid forms of timing behavior and that nearby structures, such as the hippocampus, are not necessary for learning this flexible timing task. Finally, the results identify the particular cognitive strategy employed by the animal to discriminate contexts that contain more complex temporal structure, that often exist in nature. Together these results establish a precise role of MEC in learning flexible timing behavior and demonstrate that learning is driven by context-dependent sequential neural dynamics of MEC time cells.

Introduction

The nervous system must perceive and learn the duration of events and actions to successfully guide adaptive behavior. This is true across a range of timescales, from millisecond timing which allows precise execution of timed movements, to circadian timing which mediates sleep-wake cycles (Balsam and Gallistel 2009; Buhusi and Meck 2005). During waking hours, animals heavily rely on the intermediate scale of interval timing (timing on the order of seconds to minutes) to plan and execute actions across a wide range of behavior, including foraging, mating, prey capture and avoidance (Kacelnik, Brunner, and Gibbon 1990; Marshall and Kirkpatrick 2017; Brunner et al. 1997). Numerous studies have provided insights into how the brain represents and drives interval timing behavior. The vast majority of these studies have used simple interval timing tasks in which animals discriminate and/or reproduce a single, fixed temporal interval. This body of work has demonstrated that brain circuits in the basal ganglia, frontal, and parietal cortices are necessary for learning and producing interval timing behavior, particularly for longer, supra-second to minutes time-scale durations (Matell, Meck, and Nicolelis 2003; Hinton and Meck 2004; Warren H. Meck 2006; Jin, Fujii, and Graybiel 2009; Jazayeri and Shadlen 2015; Mello, Soares, and Paton 2015; Toda et al. 2017; Bakhurin et al. 2017). Many of the identified circuits are key nodes of the procedural memory system. In contrast, medial temporal lobe (MTL) structures, including the hippocampus and entorhinal cortex, are necessary for encoding semantic and episodic memory which also requires accurate temporal coding (Tulving 1984; MacDonald et al. 2011; Eichenbaum 2014). However, there has been limited evidence to support the hypothesis that MTL brain structures play a key role in interval timing behavior (W. H. Meck, Church, and Olton 1984; Allman et al. 2014; Gladhill et al. 2022). Alternatively, it is possible that the MTL memory system does play a critical role in interval timing, but prior work has not revealed this functional role due to the use of behavioral paradigms that do not require the type of flexible learning the MTL likely evolved to mediate. Indeed, early work in animal models to demonstrate a selective deficit in learning and memory following MTL lesions was only possible after appropriate behavioral design (Mahut 1971; Mishkin 1978; Gaffan 1977; Dudchenko, Wood, and Eichenbaum 2000), despite observations in human years prior indicating these structures play a selective role in episodic memory (Scoville and Milner 1957; Milner 1965; Zola-Morgan, Squire, and Amaral 1986).

Conceptual and experimental data hint that the medial entorhinal cortex is well-suited to support interval timing within the MTL memory system (Kraus et al. 2015; Heys and Dombeck 2018; Issa et al. 2020).

Conceptually, the circuit architecture thought to drive spatially selective grid cell firing in MEC could also drive time cell activity. Mounting evidence suggests that the periodic spatial firing patterns of MEC grid cells are driven by a continuous attractor network (Burak and Fiete 2009; Yoon et al. 2013; Stensola et al. 2012; Gardner et al. 2022). Within this model framework, local recurrent synaptic connectivity generates an activity bump(s) localized on a 2D toroidal manifold. The integration of feedforward synaptic input encoding animal speed and heading direction translate this bump(s) across the manifold to produce periodic spatial firing of grid cells. This process of integrating information about animal movement to give rise to a measure of distance traveled from a start location (i.e. path integration) is strikingly similar to the computation performed by a clock. In the case of a clock, this mechanism can be simplified to integrating input with a constant mean to give rise to a measure of duration rather than distance. Prior studies provide experimental support that MEC is involved in timing, and suggest timing is supported by sequential time cell activity. However, studies have reported modest, sometimes inconsistent effects of MEC inhibition on timing behavior (Heys and Dombeck 2018; Heys et al. 2020; Dias, Ferreira, and Remondes 2021; Vo et al. 2021). We suggest the lack of a clear understanding of MEC in timing behavior stems from the use of timing tasks that do not fit the flexible learning constraints of the MTL memory system, and may instead be learned or solved though other circuits.

We therefore hypothesize that MEC has a specific role in flexible, context-dependent timing behavior, which it drives through time-locked, sequential neural firing across a population of time coding neurons. To test this hypothesis, we first developed a novel temporal delayed nonmatch to sample (tDNMS) task that requires flexible, context-dependent timing. By performing 2-photon calcium imaging as mice performed the tDNMS task, we uncovered populations of MEC time cells that fire selectively at specific moments in the timing task, and as a population, the sequence spans the entire timing epoch. Remarkably, we find that over the course of learning, these sequences become context-dependent, whereby specific populations of MEC time cells become active on particular trial types and the population dynamics shift to overrepresent later, more salient moments in the timing task. Further we find these neural dynamics are disrupted on error trials, suggesting this activity is necessary to support interval timing behavior. To affirm that MEC neural dynamics support tDNMS behavior, we chemogenetically inhibited MEC, which completely prevented mice from learning contextual timing behavior. Together these results establish a precise role of MEC in learning flexible timing behavior and demonstrate that learning is driven by context-dependent sequential neural dynamics of MEC time cells.

Results

Mice learn novel tDNMS task using flexible timing behavior

We designed a timing task with the goal of maximally engaging the MTL memory system. Due to the known dependence of delayed nonmatch to sample (DNMS) tasks on MTL regions (Mishkin 1978; Squire and Zola-Morgan 1991; Otto and Eichenbaum 1992), we adapted this structure to create a temporal delayed nonmatch to sample (tDNMS) task. In each trial of the tDNMS task, mice report whether the duration of pairs of successively presented stimuli differ. Because mice heavily rely on olfaction, we built a flow dilution olfactometer (Verhagen et al. 2007) and signaled stimuli via a single odorant (isoamyl acetate). We validated our system by ensuring that the concentration of the odorant remains constant over the course of 45 mins during a full training session, that the odor concentration can be rapidly controlled and perceived by the mice as reported through sniffing behavior (Figure S1B,C).

In each trial of the task, a water-restricted, head-fixed mouse (Figure 1A) is presented with two successive stimuli for either a short (2s) or long (5s) duration, separated by a brief 3s interstimulus interval (ISI). The tDNMS task consists of three trial types defined by each stimulus duration: short-long, long-short, and short-short trials. Using a “Go/No-Go” strategy, mice are trained to lick to report a nonmatch of durations (“Go trials”; short-long & long-short) and withhold from licking in response to matched durations (No-Go trials; short-short) (Figure 1C). Before beginning the tDNMS task, mice undergo a shaping procedure to learn the trial structure where they are only presented with nonmatched trials (Figure 1B and Figure S1D; see methods). As mice reach criteria (see Methods), mice begin the tDNMS task, where matched trials are first introduced and equally balanced across match and nonmatch trial types over each session (90 trials/session over ~45 mins). To test whether mice can learn the tDNMS task, we monitored behavioral performance in 26 mice over 8 training sessions (Figure 1D).
Mice began at chance performance on session 1, but steadily improved with training, averaging 73.16% correct responses on session 8 (27.16 $\pm$ 4.13 % change from Session 1 to Sessions 7&8; Repeated Measures ANOVA $F_{7,25} = 8.43$, $p < 0.001$).

Limiting the task to 3 trial types allowed mice to robustly learn the tDNMS task over 7-8 sessions. However, this design could potentially allow mice to learn the task through a rigid behavioral strategy. For

instance, instead of comparing stimulus durations, as intended, mice could learn to disambiguate total trial duration since match and nonmatch trials are different total durations. We therefore ran a series of control experiments to affirm that mice perform the task by attending to each odor duration. (1) By running the task without odor, we first confirmed that mice require olfactory stimuli to engage in the task (2.25 ± 1.01% correct on nonmatched trials without odor) (Figure S1E). (2) To determine if mice use a rigid strategy involving total trial duration, we manipulated the ISI in a subset of probe trials to make nonmatched and matched trials the same duration. This change did not affect performance, showing that mice use each stimulus duration and not overall trail length to perform the task (74.14 ± 6.71% correct responses on standard nonmatch trials, 80.71 ± 6.02% correct responses on nonmatch probe trials; p=0.19 in paired t-test) (Figure S1F). Together, these experiments demonstrate that mice perceive and use each stimulus duration to guide behavior. Mice use the same durations to differentially guide behavior based upon trial type, making the tDNMS task a flexible, context-dependent timing task that mice learn robustly over 7-8 training sessions.

MEC time cells fire in context-dependent trajectories during tDNMS task

To test the role of MEC in the tDNMS task we applied methods we have previously developed for large-scale cellular resolution two-photon calcium imaging in MEC (Heys et al. 2014) (Figure 2A-B). We recorded from populations of layer II MEC neurons expressing GCaMP6s (see Methods; Figure 2C-E), across 6 mice (Field-of-view 430 ± 54 μm medial to lateral by 380 ± 45 μm dorsal to ventral; depth below the surface 105 ± 8 μm) as well-trained mice performed the tDNMS task (16 ± 8 days of training; 74 ± 12% correct trial performance). Across the total population (1194 active neurons), we found that 41 ± 20% exhibited regular time-locked activity at a particular moment in each trial (Figure 2 F,G). Consistent with previous reports during interval timing behavior (Heys and Dombeck 2018), we found that different MEC "time cells" were selectively active at different delay times from the start of each trial, forming a regular temporal sequence that spanned the entire trial epoch (Figure 2F,G). During the tDNMS task, mice were free to run on a cylindrical treadmill. Since prior work has shown that many MEC neurons can encode distance travelled (Kraus et al. 2015; Campbell et al. 2021), we wondered whether the time-locked activity in MEC time cells might be better explained by distance travelled from trial on-set. In support of the idea that MEC time cells encode elapsed time in the task, and not distance travelled, we found that the vast majority of time cells displayed a smaller coefficient of variation when measuring as a function of elapsed time versus distance travelled from trial onset with CV of elapsed time: 56.9715 ± 2.1770, elapsed distance: 173.1156 ± 7.1908 (mean ± s.e.m.), p = 7.38 e-64, t(381) = -20.5897, paired t-test (Figure 2H).

To perform the tDNMS task, subjects must perceive and compare relative stimuli durations in order to determine trial type (i.e. nonmatch or match) and learn the appropriate response (i.e. Go or No-Go, respectively). We refer to the different combinations of stimuli and trial-type specific responses as "context". The robust learning and trial structure allowed us to determine whether MEC time cells might encode context in the tDNMS task. First, in well-trained mice, we asked whether MEC time cells display selective responses for specific trial types. By sorting the responses on specific trial types, we found that many MEC time cells were selectively active for only match or nonmatch trials (total context-dependent time cells = 80 % (n = 387 out of 484 total time cells), of which 25 % (n = 95) selective for match and 75 % (n = 292) selective for nonmatch) (for examples see Figure 2F: MEC time cells 3-5). Further, among the MEC time cells that were selective for nonmatch trials, we observed several distinct response profiles, with some neurons active on both trial types and some only active on the short-long or the long-short trial type.

Context-specific sequences support learning of flexible interval timing behavior

Initially, on day 1, mice are not able to accurately disambiguate context, but over several training sessions they learn to respond correctly on 70-80% of trials per session. If context-dependent MEC time cell activity supports task learning, our data should support several predictions. First, we would expect that context-dependent responses should be relatively absent on day 1, and emerge over the course of learning across sessions. Second, if context-dependent MEC time cell activity supports learning of the correct response, then the coherence of individual time cell activity and/or the regular sequential neural activation across the population should be disrupted on "error trials", when mice incorrectly report match or nonmatch.

To address our first prediction, we averaged the activity of MEC time cells for each trial type, and compared the correlations for each cell's response across trial types, before and after learning (see Methods). The results demonstrate that the correlations are significantly lower on day N compared to day 1 (day 1: 0.5017 ± 0.0347, day N: 0.3160 ± 0.0336 (mean ± s.e.m.), p = 7.8300e-05, z = 3.9495, Wilcoxon rank sum test) (Figure 3A,B). These results demonstrate that context-dependent MEC time cell activity is more limited on day 1 and develops to become more distinct over the course of learning. In the tDNMS task, the evidence

necessary to disambiguate context accumulates over the course of each trial, with several specific moments during which an "ideal observer" has sufficient information to disambiguate one trial type from another, and ultimately identify the correct trial context. We wondered whether the population dynamics of context-dependent MEC time cells might be informative about this time-dependent decision process, and provide further support that these context-dependent dynamics support learning in the tDNMS task. By sorting MEC time cells according to the time of peak activity on short-short trials, and comparing the correlation of sequences on short-short versus short-long trials, we find that the correlation significantly decreases as a function of time during the trial (significant negative correlations were observed in all plots; SS vs SL Day 1: r = -0.87, SS vs SL Day N: r = -0.95, SS vs LS Day 1: r = -0.92, SS vs LS Day N: r = -0.94, all p-values < 0.0001) (Figure 3A,C). Further, we find that over learning on Day N, the population coherence decreased in larger amount than Day 1 (comparison of correlation between Day 1 and Day N; SS vs SL: Z = 6.05, p < 0.0001, SS vs LS: Z = 2.08, p = 0.0375; Fisher r-to-z transformation). The results demonstrate that over the course of learning, the population of MEC time cells shifts on each trial type to encode later times in the trial, which correspond to moments when there is sufficient information to disambiguate the trial type (peak times on Day 1: 5.55 ± 0.17, Day N: 6.06 ± 0.16 (mean ± s.e.m.), p = 0.0013, two-sample Kolmogorov-Smirnov test; early peak proportion on Day 1: 35 % (n = 168/477), Day N: 26 % (n = 116/442), p = 0.0033, $\chi^2_{(1)} = 8.7$, chi-squared test) (Figure 3D,E). Together, these results demonstrate that context-dependent MEC time cell activity only emerges over learning, eventually displaying an over-representation at later moments in the task when it is possible to distinguish trial type.

To test our second prediction, we compared the average response for each MEC time cell for correct and error trials. At the single cell level, we observed that MEC time cells displayed more consistent activity on correct trials versus error trials, and this was true across all three trial types (Figure S2A). At the population level, we tested whether the specific sequence of MEC time cells for each trial type was less coherent on error trials (see Methods). The result show significantly higher coherence for time cells across randomly selected blocks of correct trials as compared to error trials on day N ([correlation between Correct Trials - Group A and Correct Trials - Group B: 0.5609 ± 0.0283, Correct Trials - Group A and Error Trials : 0.2991 ± 0.0526 (mean ± s.e.m.), p = 5.9980e-05, z = 4.0129, Wilcoxon signed-rank test]) (Figure 3F,G). Thus, the results testing both predictions on the emergence of context-dependent time cell activity over learning and the results on error trials provide support for the hypothesis that context-specific MEC time cell sequences support learning of flexible interval timing behavior.

<u>Does MEC time cell activity encode absolute time and/or relative time of the tDNMS task?</u> To answer this question, we recorded MEC time cells in the normal tDNMS task. Then half way through the recording session a longer ISI of 5 seconds was introduced (Figure S2C). Mice responded to the change in the ISI by delaying approach behavior and predictive licking (Figure S2D) (center of mass of velocity/licking event on normal and probe trials: velocity in S-S trial type: normal (8.05 ± 0.05) vs probe (7.98 ± 0.07), p = 0.33, z = 0.96; velocity in S-L trial type: normal (4.73 ± 0.11) vs probe (5.67 ± 0.10), p < 0.0001, z = 5.41; velocity in L-S trial type: normal (4.92 ± 0.19) vs probe (5.20 ± 0.10), p = 0.0065, z = 2.72; licking event in S-L trial type: normal (13.08 ± 0.07) vs probe (14.51 ± 0.06), p < 0.0001, z = 8.72; licking event in L-S trial type: normal (13.12 ± 0.08) vs probe (14.47 ± 0.03), p < 0.0001, z = 8.07; Wilcoxon rank sum test), indicating they perceived the difference in the trial structure during the probe trials. We found that, on average, the population of MEC time cells activity was delayed in response to the longer ISI (peak times on normal and probe trials: S-S trial types: normal (6.48 ± 0.42) vs probe (8.61 ± 0.50), p < 0.0001 z = 5.01; S-L trial types: normal (7.13 ± 0.32) vs probe (8.71 ± 0.45), p < 0.0001, z = 4.36; L-S trial types: normal (8.25 ± 0.42) vs probe (9.27 ± 0.43), p = 0.0013, z = 3.22; Wilcoxon signed-rank) (Figure S2E,F). These results suggest that rather than absolute time from trial onset, the majority of MEC time cells encode relative time (or "phase") of the tDNMS task.

<u>MEC is required to learn flexible, context-dependent timing behavior</u>

The emergence of context-dependent MEC time cells provides a potential neural dynamical mechanism that could underlie tDNMS learning. To causally test if MEC activity is necessary to learn the tDNMS task, we used a chemogenetic approach to inhibit MEC during task learning (Figure 4A; Figure S3). We first validated our approach by local injection of AAV expressing the pharmacologically selective designer Gi-coupled muscarinic receptor (hM4D) along the dorsal-ventral extent of MEC in transgenic mice with GCaMP6s expression under the CaMKIIa promoter (Figure S3; see Methods). Using in vivo two-photon Ca2+ imaging, the results show that the frequency of Ca2+ transients was reduced by 80% at 30 minutes post 1mg/kg DCZ injection compared to baseline (n=302 neurons across 2 mice; P < 0.01 – KS test) (Figure S3B). In order to test whether MEC activity

is necessary for tDNMS learning, we bilaterally injected AAV expressing hM4D across the dorsal-ventral extent of MEC (Figure 4B). Mice then underwent water restriction and shaping before beginning the tDNMS task. We monitored learning across 8 sessions of the tDNMS task and administered the DREADD agonist DCZ via I.P. injection 5 minutes prior to each session to inhibit MEC for the duration of training. As expected, control mice learned the task well within 8 days, averaging 72.76% correct responses across sessions 7-8 (Figure 4C) (Repeated Measures ANOVA $F_{7,15} = 5.09$, $p < 0.001$). In contrast, DREADD mice showed no improvement from session 1 to sessions 7-8 (Repeated Measures ANOVA $F_{7,14} = 1.18$, $p = 0.32$). Inactivation of MEC completely abolished the ability of mice to learn the tDNMS task.

To better understand the specific deficit caused by MEC inhibition, we analyzed data by trial type. We first noticed that control and DREADD mice perform well on short-long trials, starting immediately on session 1 (Figure 4E). This is likely due to learning that took place during the shaping phase of the task (before DCZ injections), as mice were presented with nonmatch trials. Interestingly, we noticed that performance on Day 1, for both control and DREADD mice, was poor on long-short nonmatch trials, even though mice were also presented with these trials during shaping. Drawing upon prior work on timing behavior (Ross, Walsh, and Grossman 1973; Schenk, Inglin, and Gyger 1983), we suspect the relatively poor performance on long-short trials was due to impulsive behavior driving mice to lick at the offset of the long odor presentation. Notably, we found that learning in the tDNMS task in control mice is largely driven by an improvement in matched trials (Figure 4E; Repeated Measures ANOVA $F_{7,15} = 5.93$, $p < 0.001$). We therefore expected DREADD mice to show impaired learning in this trial type. Interestingly, DREADD mice showed an initial improvement in matched trials over sessions 1-3, which is reflected in their overall learning curve. However, matched trial performance leveled near 50%, indicating that mice guessed whether to lick or not. While control mice clearly learned to withhold licking in matched trials, DREADD mice perseverated with licking behavior (Figure 4D). Notably, both DREADD and control mice engaged in predictive licking on both types of nonmatched trials from sessions 1-8 (Figure 4D). This indicates that MEC inhibition did not affect ability to perceive or estimate learned durations. The key behavioral difference between control and DREADD mice was that DREADD mice perseverated on rigid behavioral strategies and failed to adopt a flexible strategy to solve the task. MEC inhibition specifically prevented mice from learning to use temporal relationships, or temporal context, to flexibly guide behavior.

An alternative explanation for our results is that MEC inhibition may not affect the learning of temporal context, but rather, other aspects of behavior necessary for tDNMS performance. We therefore performed addition analyses to determine whether MEC inactivation impacted non-timing behavior. Our first concern was that MEC inactivation may impair odor perception. However, the strong performance and predictive licking shown by DREADD mice on nonmatch trials clearly indicate intact odor perception (Figure 4D & E). Our next concern was that MEC inhibition simply made mice more impulsive. Mice must refrain from licking to succeed in the task. If mice are impulsive, they would struggle to withhold even if they understood the task. To address a potential effect of differential impulsivity between control and DREADD mice, we compared the average time from trial onset to first lick for both control and DREADD mice across session 1. If MEC inhibition caused mice to be more impulsive, DREADD mice should lick earlier. This was not the case, indicating MEC inhibition did not make mice more impulsive (Figure S3C). Thus, our data confirm that MEC inhibition causes a specific deficit in learning flexible timing behavior.

<u>MEC is not necessary for ongoing tDNMS performance</u>

The emergence of context-dependent timing cells led us to test, and confirm, the hypothesis that MEC is necessary to learn flexible timing behavior. To determine whether MEC has an ongoing role in driving flexible timing behavior after learning, following 8 consecutive sessions of MEC inactivation, we took mice off DCZ and instead administered saline over sessions 9-14, then returned to DCZ administration to inhibit MEC over sessions 15-16 (Figure S4A). As expected, without MEC inhibition, DREADD mice learned the task, reaching 73.65 ± 2.9% correct responses over sessions 13-14 (Figure S4B). Interestingly, there was no difference in behavior from sessions 13-14 to 15-16, showing that MEC is not required to perform the tDNMS task after learning (see discussion) (Figure S4B).

<u>MEC is not required to learn rigid timing behavior</u>

The emergence of context-dependent MEC time cells and clear necessity of MEC activity in learning the tDNMS task support the hypothesis that MEC has a specific role in flexible timing behavior. However, an alternative possibility is MEC is necessary to learn any new timing behavior, even rigid behaviors. To disentangle these possibilities, we trained DREADD and control mice on a rigid, fixed interval task, in which a drop of water was delivered to the head-fixed mouse every 10s (Toda et al. 2017). Mice engage in predictive licking, defined by an

increase in licking leading up to reward delivery, when they learn the temporal structure of the task (Figure S4C). To test if MEC is needed to learn this simple timing task, we administered DCZ prior to each of 5 training sessions to inactivate MEC. DREADD and control mice equivalently engaged predictive licking, indicating clear knowledge of the task structure (Session 5- Control mice predictively licked on 57.76 ±7.27% of trials, DREADD mice on 70.88 ±4.39% of trials, $p = 0.15$ in unpaired t-test; Repeated Measures ANOVA Group Type x Time $F_{4,4} = 1.98$, $p = 0.11$). (Figure S4D,E). Therefore, MEC is not needed to learn rigid temporal relationships, indicating a specificity in flexible timing behavior.

Dorsal hippocampus is not necessary to learn tDNMS task

Together, our experiments demonstrate a clear and specific necessity of MEC in learning flexible timing behavior. Though we believe MEC is well-suited to drive timing behavior, downstream regions including the hippocampus have also been implicated in temporal processing, though not clearly in explicit interval timing (W. H. Meck, Church, and Olton 1984; Jacobs et al. 2013; Sabariego et al. 2019). In particular, the hippocampus contains time cells which seem to be stabilized by MEC input (Pastalkova et al. 2008; MacDonald et al. 2011; 2013; Robinson et al. 2017). As a result, we cannot be certain whether MEC neural dynamics drive timing behavior as hypothesized, or whether MEC provides temporal input to the hippocampus, which in turn supports behavior. To determine if the dorsal hippocampus is also required for tDNMS learning, we repeated our DREADD experiments, this time injecting DREADD or control virus into dorsal hippocampus instead of MEC (Figure S5A,B). Inactivating dorsal hippocampus did not affect task performance; control and DREADD mice both learned the task well, with each group averaging 74% correct responses on sessions 7-8 (Repeated Measures ANOVA Group Type x Time $F_{7,7} = 0.72$, $p = 0.65$) (Figure S5C). To confirm this negative result is not from a failure to sufficiently inactivate the hippocampus, we later trained the same group of mice used in the tDNMS task on a trace conditioning task with known hippocampal-dependence (Ahmed et al. 2020) (Figure S5D). DREADD mice showed disrupted learning in the trace conditioning paradigm, thereby confirming the null result in tDNMS learning was not simply due to unreliable inactivation of the hippocampus (First trial of last session- Control mice reduced licking 40.76 ±14.86% during trace period, DREADD reduced licking 1.17 ±6.85%; $p < 0.05$ in unpaired t-test). (Figure S5E,F). Therefore, dorsal hippocampus is not required for flexible timing behavior, suggesting that MEC is specialized to perform the computations underlying timing behavior.

Discussion

In this study we have sought to determine the specific role of MEC in interval timing by focusing considerably on behavioral design. We have taken inspiration from pioneering studies that used the delayed nonmatch to sample paradigm to give early insights into a specific role for medial temporal lobe structures in learning and memory (Mishkin 1978; Squire and Zola-Morgan 1991; Otto and Eichenbaum 1992). By developing and applying a temporal variant of this task, the results from our in vivo neurophysiological recordings and neural manipulation experiments offer insight into a special role of MEC for flexible interval timing behavior. First, we find that many individual MEC neurons (time cells) fire selectively at discrete moments during timing behavior and as a population, span the entire timing epoch with their sequential neural activation. This finding of timing activity in MEC stands in contrast to the vast majority of studies which have focused on a specialized role for MEC in navigation and spatial memory (Quirk et al. 1992; Frank, Brown, and Wilson 2000; Fyhn et al. 2004; Hafting et al. 2005; Steffenach et al. 2005; Fyhn et al. 2007; 2008; Sargolini et al. 2006; Doeller, Barry, and Burgess 2010; Yartsev, Witter, and Ulanovsky 2011; Killian, Jutras, and Buffalo 2012). In our task, mice were free to run on a cylindrical treadmill and often exhibited stereotyped running and approach behavior at specific moments when they were able to discriminate nonmatch-go and match-go trials (Figure S2D). To rule out the possibility that we were in fact measuring distance, rather than time, coding cells we made several measures that consistently demonstrate MEC time cells were in fact yoked to elapsed time, but not distance (Figure 2H). Moreover, we find that many MEC time cells fired selectively for specific nonmatch trial types (long-short vs short-long), when the running and approach behavior were identical, further suggesting timing and temporal context, were the salient behavioral variables (Figure 2F; Figure S2D). As a third measure, we also examined velocity tuning of MEC time cells. Across the population of MEC time cells there was a small, but significant correlation between the DF/F activity and velocity (0.0022 ± 0.0046 median ± SEM; $P<0.035$ Sign Rank Test) (Figure S2B). However, the distribution of correlation coefficients for MEC Time cells was not significantly different from non-Time Cells ($P=0.82$; Wilcoxon Rank Sum Test) (Figure S2B), suggesting velocity cannot account for the significant time-locked activity seen in MEC time cells. Together, with the literature on spatial navigation and a recently expanding literature demonstrating a role for MEC in nonspatial memory, data support suggests a broader role for MEC in

mnemonic function (Kraus et al. 2015; Aronov, Nevers, and Tank 2017; Robinson et al. 2017; Heys and Dombeck 2018).

A key finding of this study is that the neural dynamics of MEC time cells become context-dependent over the course of learning. Several observations provide evidence to suggest that the learned dynamics support learning of complex timing behavior. First, at specific moments in the timing task, when the animal can disambiguate temporal context, the population dynamics diverge, with different subpopulations of MEC time cells becoming active for the reminder of the trial. Second, we find that over learning, the population of MEC time cells shifts to over-represent later times in the trial, when the animal can disambiguate trial type, and thereby solve the instrumental task. Third, on error trials, when the animal mistakenly classifies the trial context, we find that the time-locked sequence of MEC time cells is disrupted. Finally, we see that this role for MEC in learning flexible interval timing behavioral may be unique. We find that mice are completely unable to learn this task with MEC inactivation. This is in line with prior work demonstrating inactivation or lesions to MEC can disrupt timing behavior (Heys et al. 2020; Dias, Ferreira, and Remondes 2021; Vo et al. 2021). Notably, the large effect we have observed in the novel tDNMS task (Cohen's d = 1.13 for the % change in performance from session 1- 7&8 for control and MEC inactivation mice), perhaps indicates that more flexible and/or complex timing behavior relies heavily on MEC compared to simple tasks where effects are small or nonexistent (further discussion below). That is, MEC is not necessary for learning more rigid timing behavior, which can likely be learned through basal ganglia structures (Matell, Meck, and Nicolelis 2003; Hinton and Meck 2004; Jin, Fujii, and Graybiel 2009; Mello, Soares, and Paton 2015; Toda et al. 2017; Bakhurin et al. 2017). While MEC is necessary for the flexible tDNMS task, we find that the dorsal hippocampus is not necessary for learning this task. Together, this suggests that MEC could play a specific role in learning flexible interval timing through regular sequential activation of context dependent MEC time cells.

Interval timing is a fundamental computation that is necessary for many adaptive behaviors and cognitive processes, including learning and memory. Yet, prior work to investigate a role for the entorhinal cortex and the hippocampus in temporal processing has been focused largely on questions of how memories evolve over time or how information is linked across disparate temporal epochs (Pastalkova et al. 2008; MacDonald et al. 2011; Cai et al. 2016; Mankin et al. 2012; Ziv et al. 2013), but not interval timing per se. Our novel timing paradigm used in this study offers insights not only into neural dynamics, but also the cognitive strategy that may support the learning of flexible timing behavior. In our version of the tDNMS task, mice were presented with three trial types: short-long and long short, which served as nonmatch-go context, and short-short trials, which served as the match-no-go context. Importantly, long-long match trials are absent in this paradigm, and the long duration stimuli are therefore only presented on nonmatch-go trials. Using this three trial type structure permits subjects to employ one of several potential cognitive strategies to discriminate match-no-go and nonmatch-go context on each trial. These different cognitive strategies may differ in their complexity and ability to flexibly generalize. Notably, each strategy makes specific predictions regarding the timing behavior in the standard task and different predictions for how mice should respond to particular types of trial structure manipulations (i.e. probes). Strategy 1: In the most rigid and simple strategy, mice could learn to selectively identify long duration stimuli as a go cue, and wait to respond until the 2nd stimuli offset. This strategy only requires timing for a single interval and predicts that mice should not predictively lick near trial offset times. Strategy 2: Since the nonmatch trials are longer in total duration than the match trials, mice employ a different cognitive strategy to time the full trial interval, and ignore the relative intervals in the first and second stimuli. Again, this strategy only requires timing a single interval. This strategy predicts that mice should withhold licking on a small random subset of probe trials where the interstimulus interval is changed such that the total duration on nonmatch is the same as prior for the match trials. Strategy 3: Mice may also use the strategy of identifying long stimuli as a go cue, and also time the duration of each consecutive stimuli to predict when to respond (lick) or withhold response on nonmatch or match trials, respectively. In this case, mice actively time multiple stimuli durations on each trial, but may not necessarily be comparing their durations to decide to respond or not. A key prediction of this strategy is that mice display predictive licking on nonmatch trials, especially on the long-short trials where the go cue has already been discriminated early in the trial. Further, if the mice are timing the second stimuli on long-short trials, then manipulations of the interstimulus interval on these trials should not change the distribution of predictive licking aligned to the start of the second stimulus. Strategy 4: mice may also learn a general rule to encode both stimuli durations, and compare at the end of the trial to employ the go-nonmatch/No-go-match rule, which is perhaps the most abstract strategy between these four. In this case, mice should not predictively lick on long-short trials, as they should not be classifying these trials as nonmatch until after the stimuli has ended. Together, the data showing that 1) manipulating the interstimulus interval (Figure S1 and Figure S2D) does not change the timing of predictive licking to reward or decrease % correct on probe trials, 2) predictive licking is present, especially

on long-short trials (Figure 4) and 3) the distribution of predictive lick times, to reward delivery, does not change on interstimulus interval probe trials (Figure S2D), suggests that mice are using strategy 3. We argue that is a relatively complex cognitive process that requires encoding a hierarchical structure between multiple duration stimuli on each trial and learning to respond at specific predicted moments in this task structure. This strategy is more complex than strategy 1 or 2, which could be solved with a simpler decision structure, but likely not as abstract as a true nonmatch to sample comparison as required for strategy 4. In future work, it is possible that by designing tasks that require even more flexible and/or abstract timing strategies that MEC would be required for ongoing performance, or perhaps dHPC could be required for normal learning.

MEC is positioned within a larger network of medial temporal lobe structures, including the hippocampus, entorhinal, peri and post-rhinal cortices. How do our findings fit in the context of this larger memory system? The structure of our task allowed us to observe the emergence of contextual time cells that support a specific necessity of MEC in learning flexible, context-dependent timing. Context-dependent time cells have previously been reported in the hippocampus (MacDonald et al. 2011; 2013; Salz et al. 2016). However, our finding that dHPC is not necessary for tDNMS learning suggests such cells are not needed for tDNMS performance. Rather, MEC may directly project to regions such as the prefrontal cortex (Delatour and Witter 2002; Witter 2003) to mediate decision making and motor output. Although our trace conditioning experiment provides confidence that our null result was not from a failure to inactivate dHPC, it remains possible that with broader hippocampal inactivation, a deficit would be revealed. To date, it remains unclear how the hippocampus contributes to interval timing behavior: some studies report a necessity (for instance (W. H. Meck, Church, and Olton 1984)), others do not (for instance(Dietrich and Allen 1998)), and others report a necessity only for certain durations (Jacobs et al. 2013; Palombo, Keane, and Verfaellie 2015). A key future direction will be to establish a more precise contribution of the hippocampus to timing. Additionally, while our work focused on MEC, time-locked activity has also been recorded from lateral entorhinal cortex (Tsao et al. 2018). It remains unclear whether or how MEC, LEC, and HPC time-tuned neurons are related. More work is clearly required to establish how the MTL memory system performs timing; however, our study demonstrates that MEC time cells are a key component. Our results add evidence that the role of MEC in memory extends beyond spatial encoding and may lead to a deeper understanding of MEC circuit function.

Since the discovery of spatially selective MEC grid cells there has been a strong focus on the role of MEC in navigation and spatial memory. This research program has been remarkably productive, and although there still are some outstanding questions remaining, this line of research has given substantial insight into the circuit mechanisms that underlie grid cell firing. Namely, there is strong support for a CAN that is mediated through structured local recurrent synaptic connectivity of MEC neurons (Burak and Fiete 2009; Yoon et al. 2013; Stensola et al. 2012; Gardner et al. 2022). A key feature to this model is that the network integrates synaptic input coding for animal heading direction and velocity, thereby driving sequential activity of a population of grid cells, each coding for different spatial phase(s) within an environment. This process is mathematically equivalent to path integration (Burak and Fiete 2009; Issa and Zhang 2012), giving rise to a measure of distance travelled from a start location. We find this computation conspicuously similar to that of a clock, which rather than a measure of distance, can integrate a constant input to give rise to a measure of duration from a start time. When animals are moving through space, their distance and duration travelled are proportional via velocity. Given the environmental context, it could be optimal to estimate different features of elapsed time and/or distance travelled. For example, to minimize the path/duration to home from a patch location, animals might sometimes use the shortest, most direct path while other times it might be optimal to compute the minimal duration across multiple routes. We suspect that during timing, the sequential activity of MEC time cells is driven through the similar continuous attractor network dynamics, that may have evolved for similar and often overlapping navigation processes across time and space. Such overlap could indicate that MEC neurons may serve as a general integration circuit, calculating either distance or time based upon relative behavioral demands.

Materials and Methods

Surgery and Behavior

AAV injections: To inhibit MEC, C57-BL6 mice (n = 40 mice: 20 male & 20 female; postnatal 2-3 months) were injected bilaterally with pAAV-CaMKIIa-hM4D(Gi)-mCherry (Addgene: AAV8; 2.40 x 10^{13} GC/mL; diluted 1:1 in PBS) or pAAV-CaMKIIa-mCherry (Addgene: AAV1; 1.40E x 10^{13} GC/mL; diluted 1:1 in PBS). A Nanoject III Injector (Drummond) was used to inject 80nL of virus (divided into 4x20nL injections; injection rate of 10nL/s) at 6 sites in each hemisphere. Injections were targeted at 2.9mm lateral from bregma and 0.15mm rostral of the

transverse sinus; at 3.3mm lateral from bregma and 0.15mm rostral of the transverse sinus; and at 3 depths (1.2mm, 1.6mm, and 2mm) from the dorsal surface of the brain. To inhibit the dorsal hippocampus, the same protocol was used to perform bilateral injections (n = 36 mice: 18 male & 18 female; postnatal 2-3 months). Hippocampal injections were instead targeted at 4 sites per hemisphere. 2 sites were positioned 1.8mm posterior of bregma: 1.2mm lateral from bregma at a depth 1.3mm from the dorsal surface of the brain & 2mm lateral from bregma at a depth 1.7mm. The remaining 2 sites were positioned 2.3mm posterior of bregma: 1.75mm lateral from bregma at a depth of 1.3mm; 2.6mm lateral of bregma at a depth of 2.1mm.

MEC microprism implant: All experiments were approved and conducted in accordance with the University of Utah Animal Care and Use Committee. Methods for MEC microprism implant have been described previously(Heys, Rangarajan, and Dombeck 2014; Heys and Dombeck 2018). Briefly, 6 mice (5m and 1f) C57-BL6 mice (~P70) were anesthetized using 1–2% isoflurane. An approximately rectangular craniotomy was made over the dorsal surface of the cortex (above MEC) and cerebellum with corners positioned as follows: (i) ~2.1 mm lateral of bregma, ~4.5 mm caudal of bregma (~300–500 μm rostral of the transverse sinus); (ii) ~4.5 mm lateral of bregma, ~4.5 mm caudal of bregma (~300–500 μm rostral of the transvers sinus); (iii) ~2.1 mm lateral of bregma, ~7.75–8 mm caudal of bregma (~3.25–3.5 mm caudal of the transverse sinus); and (iv) ~4.5 mm lateral of bregma, ~7.75–8 mm caudal of bregma (~3.25–3.5 mm caudal of the transverse sinus). After the skull was removed, a portion of the cerebellum was aspirated to expose the caudal surface of the cortex. The tentorium separating the cerebellum and cortex was carefully removed, leaving the dura of the cortex completely intact. A microprism (right-angle prism with 1.5-mm side length and reflective enhanced aluminum coating on the hypotenuse, Tower Optical) was mounted on a custom stainless-steel mount (using UV-curable adhesive, Norland). This assembly was then positioned by aligning the front face of the microprism parallel to the caudal surface of the MEC and aligning the top surface of the microprism perpendicular to the (eventual) axis of excitation light propagation. A thin layer of Kwik-Sil was applied to the caudal MEC surface before microprism implantation to fill the void between the brain and the front surface of the microprism. The microprism and mount were rigidly held in place and the craniotomy sealed by application of a thin layer of Metabond to all exposed sides of the microprism (except the top surface of the prism) and mount and on any exposed skull or brain. A titanium headplate (9.5 mm × 38 mm) was then attached to the dorsal surface of the skull, centered upon and aligned parallel to the top face of the microprism. A titanium ring (27-mm outer diameter and 12.5-mm inner diameter, with a 3-mm high edge) was then attached to the top surface of the headplate, centered around the microprism, and the area between the craniotomy and the inner edge of the metal ring was covered with opaque dental cement (Metabond, Parkell, made opaque by adding 0.5 g of carbon powder, Sigma Aldrich).

Experimental Setup: Mice were head-fixed over a cylindrical treadmill in a dark enclosure. After being head-fixed, an odor nozzle and lick spout were placed near the mouse. Odorized air was delivered using a flow dilution olfactometer (Verhagen et al. 2007). The olfactometer consisted of two streams of air: a carrier stream (0.9 L/min) and an odorized stream (50 mL/min) which carried isoamyl acetate (2% isoamyl acetate in mineral oil; odorant from Cole-Parmer, 99+%). The two streams combined, and a solenoid valve was used to direct odorized air either to the odor nozzle or to a vacuum (1.8 L/min). Odor delivery was validated through use of a photoionization detector (PID). Licking was monitored throughout each training session and was detected using a capacitance sensor (SparkFun Capacitive Touch - AT42QT1010) with an electrode positioned on the lick spout. A solenoid valve was used to deliver water (~6 ul per drop) via the lick spout when appropriate. All experimental paradigms were automated and controlled though the use of an Ardunio Uno, and data collection was performed using a Picoscope oscilloscope (PICO4824, Pico Technology, v6.13.2) sampled at 1kHZ.

Behavioral Training: After recovering from surgery, mice began water restriction (~1mL of water per day). Once mice reached ~85% of their initial weight, they began pre-training for the tDNMS task. Mice were first acclimated to the experimental setup though a habituation phase. During habituation, series of 50 drops of water (3s apart) were delivered to the mouse (3-6 series of drops per session). Habituation ended after mice licked to consume $\geq$80% of water drops in a series. Following habituation, mice began 3 phases of shaping: Shaping 1, Shaping 2, and Shaping 3. Shaping followed the same trial structure of the tDNMS task; however, only nonmatched trials were used. Each trial consisted of a flash of green light to alert mice the trial was about to begin, the first odor, an interstimulus interval, the second odor, and a response window. Trials were separated by a random intertrial interval (ranging from 16-24s). In Shaping 1, a drop of water was automatically delivered 0.25s after second odor offset in each trial. Once mice licked to consume drops in $\geq$80% of trials, they progressed to Shaping 2. Probe trials were introduced in Shaping 2, in which the mouse had to lick within a 3s response window following second

odor offset to trigger a reward. If the mouse successfully triggered reward, the next trial was another probe trial. If the mouse failed to trigger a reward in a probe trial, the following trial was automatically rewarded, after which the mouse was given another probe trial. Training on this phase continued until mice licked to earn reward in ≥20 consecutive trials. Mice then began Shaping 3, which had the same probe trial format as Shaping 2. However, in addition to licking in the response window, mice were also required to withhold licking during the first odor and interstimulus interval (ISI) to trigger reward delivery. Training on this phase continued until mice reached 2 consecutive sessions of ≥ 20 consecutive rewarded trials, after which they began the tDNMS task. Some mice failed to reach this benchmark yet routinely performed above chance on probe trials; they instead began the tDNMS task after reaching ≥ 80% correct performance on probe trials. Following shaping, mice began the tDNMS task, where matched trials were introduced. Matched and non-matched trials were included in a pseudo-random manner and balanced so that half of trials were matched and half were nonmatched. Mice were rewarded in nonmatched trials if they withheld licking during the first odor and ISI and licked within the 3s response window following second odor offset. Mice received no reward in matched trials and were punished for licking in the response window by an increased ITI (+12s). Mice were trained for 1 session per day, with each session consisting of 100 trials for shaping, or 90 trials for the tDNMS task. Mice were trained at least 5 days/week during pretraining and 7 days/week during the tDNMS task.

Some mice were also trained on a Fixed Interval (FI) or Trace Conditioning (TC) task following tDNMS training. The same experimental apparatus was used for these tasks. In each session of the FI task, a (~6ul) drop of water was delivered to the head-fixed mouse every 10s (150 drops per session). Mice were trained for 1 session per day and completed 5 training sessions on the FI task. For the TC task, mice were habituated for 1 day on an instrumental licking paradigm, in which each lick was rewarded with a small drop of water. All mice licked consistently for the ~5 minute duration of this habituation session. The following day, mice began the TC task. The TC task began with a baseline period (≥ 60s), after which the conditioned stimulus (CS), a 20s green light, was presented. The CS was followed by a 15s trace period, after which animals received 5x air puffs (spaced 1s apart) delivered to the snout. Each air puff was accompanied by noise generated by a buzzer. Mice earned water each time they licked during the duration of the TC sessions (except during air puff delivery). In all behavioral paradigms (tDNMS, FI and TC) mice were free to run on a cylindrical treadmill (60 cm in circumference and cm in width). Mouse velocity was measured using rotary encoder (E2-5000, US Digital).

Two-photon imaging of MEC neurons: After mice were pretrained on the tDNMS task (14.5 ± 3.9 days for pretraining), we began two-photon laser resonance scanning of populations of neurons expressing GCaMP6s through the microprism using a Neurolabware microscope. Data was acquired with an 8 kHz resonant scanner, images were collected at a frame rate of 30 Hz with bidirectional scanning through and Scanbox software was used for microscope control and acquisition. A Ti:Sapphire laser (Discovery with TPC, Coherent) light at 920 nm was used as the excitation source with average power measured at the sample (after the objective; 20×/0.45 NA air immersion objective (LUCPanFL, Olympus) with correction collar set at 1.25) was 50-120 mW. Imaging data was recorded using a PicoScope Oscilloscope (PICO4824, Pico Technology, v6.13.2) sampled at 1kHZ to synchronize with behavior.

Data analysis

General:
Imaging data was analyzed on a IBuyPower Intel Core with Windows10 and custom software written in Matlab (2018b). No statistical methods were used to predetermine sample sizes. Sample sizes were based on reliably measuring experimental parameters while remaining in compliance with ethical guidelines to minimize the number of animals used. Repeated Measures ANOVA, paired t-test, Wilcoxon rank sum test, two-sample Kolmogorov-Smirnov test, chi-squared test, Wilcoxon signed-rank tests were used to test for statistical significance when appropriate, and all statistical tests were two-sided unless stated otherwise. For tests assuming normality, data distributions were assumed to be normal, but this was not formally tested. Experimenters were blinded during data collection of MEC - DREADD inactivation experiments in the tDNMS task and during the hippocampus inactivation experiments in the tDNMS task (experimenters were not blinded for fixed interval or trace conditioning experiments). All data in the text and figures are labeled as either mean ± s.d. or mean ± s.e.m.

Behavioral Performance: Performance on the tDNMS task was analyzed by determining the percent of trials in which mice behaved correctly. Correct nonmatched trials were defined as those in which mice withheld licking during the first odor and ISI and licked in the 3s response window following second odor offset to trigger reward. Correct matched trials were defined as those in which mice withheld licking for the duration of the trial. Mice that met the criteria to advance beyond shaping and begin the tDNMS task were included in analysis. However, a subset of mice were removed from analysis due to: a failure to retain the task structure learned in shaping (performance >3 SD below the mean on tDNMS session 1, n =1 mouse), headplate falling off (n = 2 mice), rig malfunction (n = 8 mice in the hippocampal tDNMS experiments due to malfunction of one rig), or lack of virus expression (n = 2 mice). Though most behavior is analyzed as % correct trials, licking behavior was further examined in some instances. Lick events were defined as samples (sampling rate of 1000Hz) in which the capacitance sensor detected a signal. Lick events were binned in 0.25s bins for analysis. For tDNMS behavior, any licking following reward delivery was removed, then licking was normalized relative to the maximum within a session. Lick events were also used to examine performance in the Fixed Interval (FI) and Trace Conditioning (TC) tasks. Performance on the FI task is measured as the % of trials in which mice engaged in predictive licking, where predictive licking is defined as an increase in lick events (determined by a significantly positive slope) in the 5s preceding reward delivery. Performance on the TC task is determined by examining the number of lick events during the 20s conditioned stimulus (CS), normalized to the 20s baseline immediately prior to the stimulus.

Image processing, ROI selection, and transient analysis:

In vivo two-photon data sets were acquired during the tDNMS task (60,000 frames per session). Movies were first motion corrected using whole-frame cross-correlation, as described previously (Heys et al 2014), and the motion-corrected time-series was used for all subsequent analysis. Regions of interest (ROIs) were defined using Suite2P v0.10.1 (Pachitariu et al. 2016). Significant Ca2+ DF/F transients were identified using methods described in (Dombeck et al. 2010; Heys, Rangarajan, and Dombeck 2014; Heys and Dombeck 2018).

Defining time cells in the tDNMS task:

Cells with significant tuning at a specific time point during trials were defined based on mutual information(Skaggs, W 1992; Climer and Dombeck 2021). Before computing mutual information, Ca^{2+} signals were normalized in each trial by dividing their peak dF/F value to prevent that one or two large transients determine a cell's activity pattern. Then, dF/F values averaged across correct trials, and mutual information of averaged dF/F was obtained using following equation for each trial type (e.g., short-short, short-long, long-short):

$$Mutual\ information\ = \sum_i p_i \lambda_i \log_2 \frac{\lambda_i}{\lambda}$$

where i denotes bin, p_i is occupancy rate in ith bin, λ_i is dF/F at ith bin, and λ is mean dF/F. To test whether the mutual information is sufficiently higher than that from random activity, dF/F in each trial was circularly shifted in random amount, and mutual information was computed with shuffled data. Shuffling was repeated 1,000 times. P-value was defined as a proportion of shuffled mutual information greater or equal to a real mutual information. Cells were classified as time cells if *i*) mean dF/F > 0.03 and *ii*) p-value of mutual information. < 0.01.

Comparing correlation between match and mismatch trial types across day 1 to day N
Time cells in either short-short or short-long trial types were selected, and the Pearson correlation coefficient between these two trial types was calculated in each cell. The same procedure was performed using time cells in either short-short and long-short trial types. All correlation coefficients were pooled and compared between Day 1 and Day N using Wilcoxon rank sum test.

Comparing correlation between match and mismatch trial types across time phase in trials
Time cells in either short-short or short-long trial types were selected. Population vectors were constructed from dF/F of all selected cells at each time bin. Then, the Pearson correlation coefficient between the population vectors of short-short trial type and their corresponding bin's population vectors of short-long trial type were computed. The same procedure was repeated for the time cells in either short-short or long-short trial types.

Measuring activity coherence in error trials
Due to the low number of error trials in short-long and long-short trial types, this analysis was only applied to short-short trial type. For each cell's activity, correct trials were divided into two groups using a random subset of trials (Correct A and Correct B). The number of trials assigned to Correct B was set to match the number of error trials. Cell activity was sorted according to the sequence in correct A group and correlations for each cell's activity were computed for correct A versus correct B (blue) and correct A versus error (red). Trial random sampling was repeated 1,000 times to get a distribution of correlation coefficients. Then, the mean values of these correlation coefficients were taken as the cell's correlation coefficient values.

Comparing variance in time and distance dimension
The dF/F of time cells were redrawn as a function of elapsed running distance from the trial initiation light being turned on. In each trial, the peak location of dF/F was detected in distance dimension. The variance of the peak locations was measured by coefficient of variation. Coefficient of variation is a ratio of the standard deviation to the mean, which gives a standardized measure of dispersion and is used to compare variations between different scales or dimensions. The same procedure was repeated as a function of elapsed time from the light being turned on. Then, coefficient of variation of time cells were compared between distance and time dimension by Student's Paired T-test.

Histology
Following behavioral experiments, mice were euthanized and the brain was removed and fixed in 4% PFA in 0.1M PBS for ~24 hours. The brains were then rinsed 3x with 0.1M PBS, then stored in PBS for 1+ days before the tissue was sectioned in 50-100 micron sagittal or coronal slices using a vibrating microtome. Free floating slices were then incubated in 0.1M PBS with 0.1% Triton-X for 15 minutes, washed with 0.1M PBS and incubated for 3 hours in a 25:1 solution of 0.1M PBS with 435/455 blue or 530/615 red fluorescent Nissl stain (Invitrogen). Brain sections were imaged and stitched using a VS200 Virtual Slide fluorescence microscope (Olympus) with a 10x OFN26.5, NA 0.40 objective (Olympus).

References

Allman, Melissa J., Sundeep Teki, Timothy D. Griffiths, and Warren H. Meck. 2014. "Properties of the Internal Clock: First- and Second-Order Principles of Subjective Time." *Annual Review of Psychology* 65: 743–71. https://doi.org/10.1146/annurev-psych-010213-115117.

Aronov, Dmitriy, Rhino Nevers, and David W. Tank. 2017. "Mapping of a Non-Spatial Dimension by the Hippocampal-Entorhinal Circuit." *Nature* 543 (7647): 719–22. https://doi.org/10.1038/nature21692.

Bakhurin, Konstantin I., Vishwa Goudar, Justin L. Shobe, Leslie D. Claar, Dean V. Buonomano, and Sotiris C. Masmanidis. 2017. "Differential Encoding of Time by Prefrontal and Striatal Network Dynamics." *The Journal of Neuroscience: The Official Journal of the Society for Neuroscience* 37 (4): 854–70. https://doi.org/10.1523/JNEUROSCI.1789-16.2016.

Balsam, Peter D., and C. Randy Gallistel. 2009. "Temporal Maps and Informativeness in Associative Learning." *Trends in Neurosciences* 32 (2): 73–78. https://doi.org/10.1016/j.tins.2008.10.004.

Brunner, D., S. Fairhurst, G. Stolovitzky, and J. Gibbon. 1997. "Mnemonics for Variability: Remembering Food Delay." *Journal of Experimental Psychology. Animal Behavior Processes* 23 (1): 68–83. https://doi.org/10.1037//0097-7403.23.1.68.

Buhusi, Catalin V., and Warren H. Meck. 2005. "What Makes Us Tick? Functional and Neural Mechanisms of Interval Timing." *Nature Reviews. Neuroscience* 6 (10): 755–65. https://doi.org/10.1038/nrn1764.

Burak, Yoram, and Ila R. Fiete. 2009. "Accurate Path Integration in Continuous Attractor Network Models of Grid Cells." *PLoS Computational Biology* 5 (2): e1000291. https://doi.org/10.1371/journal.pcbi.1000291.

Cai, Denise J., Daniel Aharoni, Tristan Shuman, Justin Shobe, Jeremy Biane, Weilin Song, Brandon Wei, et al. 2016. "A Shared Neural Ensemble Links Distinct Contextual Memories Encoded Close in Time." *Nature* 534 (7605): 115–18. https://doi.org/10.1038/nature17955.

Campbell, Malcolm G., Alexander Attinger, Samuel A. Ocko, Surya Ganguli, and Lisa M. Giocomo. 2021. "Distance-Tuned Neurons Drive Specialized Path Integration Calculations in Medial Entorhinal Cortex." *Cell Reports* 36 (10): 109669. https://doi.org/10.1016/j.celrep.2021.109669.

Climer, Jason R., and Daniel A. Dombeck. 2021. "Information Theoretic Approaches to Deciphering the Neural Code with Functional Fluorescence Imaging." *ENeuro* 8 (5): ENEURO.0266-21.2021. https://doi.org/10.1523/ENEURO.0266-21.2021.

Delatour, B., and M. P. Witter. 2002. "Projections from the Parahippocampal Region to the Prefrontal Cortex in the Rat: Evidence of Multiple Pathways." *The European Journal of Neuroscience* 15 (8): 1400–1407. https://doi.org/10.1046/j.1460-9568.2002.01973.x.

Dias, Marcelo, Raquel Ferreira, and Miguel Remondes. 2021. "Medial Entorhinal Cortex Excitatory Neurons Are Necessary for Accurate Timing." *The Journal of Neuroscience: The Official Journal of the Society for Neuroscience* 41 (48): 9932–43. https://doi.org/10.1523/JNEUROSCI.0750-21.2021.

Dietrich, Arne, and Joseph D. Allen. 1998. "Functional Dissociation of the Prefrontal Cortex and the Hippocampus in Timing Behavior." *Behavioral Neuroscience* 112 (5): 1043–47. https://doi.org/10.1037/0735-7044.112.5.1043.

Doeller, CF, C Barry, and N Burgess. 2010. "Evidence for Grid Cells in a Human Memory Network." *Nature* 463: 657–61.

Dombeck, Daniel A., Christopher D. Harvey, Lin Tian, Loren L. Looger, and David W. Tank. 2010. "Functional Imaging of Hippocampal Place Cells at Cellular Resolution during Virtual Navigation." *Nature Neuroscience* 13 (11): 1433–40. https://doi.org/10.1038/nn.2648.

Dudchenko, P. A., E. R. Wood, and H. Eichenbaum. 2000. "Neurotoxic Hippocampal Lesions Have No Effect on Odor Span and Little Effect on Odor Recognition Memory but Produce Significant Impairments on Spatial Span, Recognition, and Alternation." *The Journal of Neuroscience: The Official Journal of the Society for Neuroscience* 20 (8): 2964–77. https://doi.org/10.1523/JNEUROSCI.20-08-02964.2000.

Eichenbaum, Howard. 2014. "Time Cells in the Hippocampus: A New Dimension for Mapping Memories." *Nature Reviews. Neuroscience* 15 (11): 732–44. https://doi.org/10.1038/nrn3827.

Frank, L. M., E. N. Brown, and M. Wilson. 2000. "Trajectory Encoding in the Hippocampus and Entorhinal Cortex." *Neuron* 27 (1): 169–78. https://doi.org/10.1016/s0896-6273(00)00018-0.

Fyhn, Marianne, Torkel Hafting, Alessandro Treves, May-Britt Moser, and Edvard I. Moser. 2007. "Hippocampal Remapping and Grid Realignment in Entorhinal Cortex." *Nature* 446 (7132): 190–94. https://doi.org/10.1038/nature05601.

Fyhn, Marianne, Torkel Hafting, Menno P. Witter, Edvard I. Moser, and May-Britt Moser. 2008. "Grid Cells in Mice." *Hippocampus* 18 (12): 1230–38. https://doi.org/10.1002/hipo.20472.

Fyhn, Marianne, Sturla Molden, Menno P. Witter, Edvard I. Moser, and May-Britt Moser. 2004. "Spatial Representation in the Entorhinal Cortex." *Science (New York, N.Y.)* 305 (5688): 1258–64. https://doi.org/10.1126/science.1099901.

Gaffan, David. 1977. "Monkeys' Recognition Memory for Complex Pictures and the Effect of Fornix Transection." *Quarterly Journal of Experimental Psychology* 29 (3): 505–14. https://doi.org/10.1080/14640747708400626.

Gardner, Richard J., Erik Hermansen, Marius Pachitariu, Yoram Burak, Nils A. Baas, Benjamin A. Dunn, May-Britt Moser, and Edvard I. Moser. 2022. "Toroidal Topology of Population Activity in Grid Cells." *Nature* 602 (7895): 123–28. https://doi.org/10.1038/s41586-021-04268-7.

Gladhill, Keri Anne, Eva Marie Robinson, Candice Stanfield-Wiswall, Farah Bader, and Martin Wiener. 2022. "Anchors for Time, Distance, and Magnitude in Virtual Movements." Preprint. Neuroscience. https://doi.org/10.1101/2022.09.12.507649.

Hafting, Torkel, Marianne Fyhn, Sturla Molden, May-Britt Moser, and Edvard I. Moser. 2005. "Microstructure of a Spatial Map in the Entorhinal Cortex." *Nature* 436 (7052): 801–6. https://doi.org/10.1038/nature03721.

Heys, James G., and Daniel A. Dombeck. 2018. “Evidence for a Subcircuit in Medial Entorhinal Cortex Representing Elapsed Time during Immobility.” *Nature Neuroscience* 21 (11): 1574–82. https://doi.org/10.1038/s41593-018-0252-8.

Heys, James G., Krsna V. Rangarajan, and Daniel A. Dombeck. 2014. “The Functional Micro-Organization of Grid Cells Revealed by Cellular-Resolution Imaging.” *Neuron* 84 (5): 1079–90. https://doi.org/10.1016/j.neuron.2014.10.048.

Heys, James G., Zihan Wu, Anna Letizia Allegra Mascaro, and Daniel A. Dombeck. 2020. “Inactivation of the Medial Entorhinal Cortex Selectively Disrupts Learning of Interval Timing.” *Cell Reports* 32 (12): 108163. https://doi.org/10.1016/j.celrep.2020.108163.

Hinton, Sean C., and Warren H. Meck. 2004. “Frontal-Striatal Circuitry Activated by Human Peak-Interval Timing in the Supra-Seconds Range.” *Brain Research. Cognitive Brain Research* 21 (2): 171–82. https://doi.org/10.1016/j.cogbrainres.2004.08.005.

Issa, John B., Gilad Tocker, Michael E. Hasselmo, James G. Heys, and Daniel A. Dombeck. 2020. “Navigating Through Time: A Spatial Navigation Perspective on How the Brain May Encode Time.” *Annual Review of Neuroscience* 43 (July): 73–93. https://doi.org/10.1146/annurev-neuro-101419-011117.

Issa, John B., and Kechen Zhang. 2012. “Universal Conditions for Exact Path Integration in Neural Systems.” *Proceedings of the National Academy of Sciences of the United States of America* 109 (17): 6716–20. https://doi.org/10.1073/pnas.1119880109.

Jacobs, Nathan S., Timothy A. Allen, Natalie Nguyen, and Norbert J. Fortin. 2013. “Critical Role of the Hippocampus in Memory for Elapsed Time.” *The Journal of Neuroscience: The Official Journal of the Society for Neuroscience* 33 (34): 13888–93. https://doi.org/10.1523/JNEUROSCI.1733-13.2013.

Jazayeri, Mehrdad, and Michael N. Shadlen. 2015. “A Neural Mechanism for Sensing and Reproducing a Time Interval.” *Current Biology: CB* 25 (20): 2599–2609. https://doi.org/10.1016/j.cub.2015.08.038.

Jin, Dezhe Z., Naotaka Fujii, and Ann M. Graybiel. 2009. “Neural Representation of Time in Cortico-Basal Ganglia Circuits.” *Proceedings of the National Academy of Sciences of the United States of America* 106 (45): 19156–61. https://doi.org/10.1073/pnas.0909881106.

Kacelnik, Alejandro, Dani Brunner, and John Gibbon. 1990. “Timing Mechanisms in Optimal Foraging: Some Applications of Scalar Expectancy Theory.” In *Behavioural Mechanisms of Food Selection*, edited by Roger N. Hughes, 61–82. Berlin, Heidelberg: Springer Berlin Heidelberg. https://doi.org/10.1007/978-3-642-75118-9_4.

Killian, Nathaniel J., Michael J. Jutras, and Elizabeth A. Buffalo. 2012. “A Map of Visual Space in the Primate Entorhinal Cortex.” *Nature* 491 (7426): 761–64. https://doi.org/10.1038/nature11587.

Kraus, Benjamin J., Mark P. Brandon, Robert J. Robinson, Michael A. Connerney, Michael E. Hasselmo, and Howard Eichenbaum. 2015. “During Running in Place, Grid Cells Integrate Elapsed Time and Distance Run.” *Neuron* 88 (3): 578–89. https://doi.org/10.1016/j.neuron.2015.09.031.

MacDonald, Christopher J., Stephen Carrow, Ryan Place, and Howard Eichenbaum. 2013. “Distinct Hippocampal Time Cell Sequences Represent Odor Memories in Immobilized Rats.” *The Journal of Neuroscience: The Official Journal of the Society for Neuroscience* 33 (36): 14607–16. https://doi.org/10.1523/JNEUROSCI.1537-13.2013.

MacDonald, Christopher J., Kyle Q. Lepage, Uri T. Eden, and Howard Eichenbaum. 2011. “Hippocampal ‘Time Cells’ Bridge the Gap in Memory for Discontiguous Events.” *Neuron* 71 (4): 737–49. https://doi.org/10.1016/j.neuron.2011.07.012.

Mahut, Helen. 1971. “Spatial and Object Reversal Learning in Monkeys with Partial Temporal Lobe Ablations.” *Neuropsychologia* 9 (4): 409–24. https://doi.org/10.1016/0028-3932(71)90005-4.

Mankin, Emily A., Fraser T. Sparks, Begum Slayyeh, Robert J. Sutherland, Stefan Leutgeb, and Jill K. Leutgeb. 2012. “Neuronal Code for Extended Time in the Hippocampus.” *Proceedings of the National Academy of Sciences of the United States of America* 109 (47): 19462–67. https://doi.org/10.1073/pnas.1214107109.

Marshall, Andrew T., and Kimberly Kirkpatrick. 2017. “Reinforcement Learning Models of Risky Choice and the Promotion of Risk-Taking by Losses Disguised as Wins in Rats.” *Journal of Experimental Psychology. Animal Learning and Cognition* 43 (3): 262–79. https://doi.org/10.1037/xan0000141.

Matell, Matthew S., Warren H. Meck, and Miguel A. L. Nicolelis. 2003. “Interval Timing and the Encoding of Signal Duration by Ensembles of Cortical and Striatal Neurons.” *Behavioral Neuroscience* 117 (4): 760–73. https://doi.org/10.1037/0735-7044.117.4.760.

Meck, W. H., R. M. Church, and D. S. Olton. 1984. “Hippocampus, Time, and Memory.” *Behavioral Neuroscience* 98 (1): 3–22. https://doi.org/10.1037//0735-7044.98.1.3.

Meck, Warren H. 2006. “Neuroanatomical Localization of an Internal Clock: A Functional Link between Mesolimbic, Nigrostriatal, and Mesocortical Dopaminergic Systems.” *Brain Research* 1109 (1): 93–107. https://doi.org/10.1016/j.brainres.2006.06.031.

Mello, Gustavo B. M., Sofia Soares, and Joseph J. Paton. 2015. “A Scalable Population Code for Time in the Striatum.” *Current Biology: CB* 25 (9): 1113–22. https://doi.org/10.1016/j.cub.2015.02.036.

Milner, Brenda. 1965. “Visually-Guided Maze Learning in Man: Effects of Bilateral Hippocampal, Bilateral Frontal, and Unilateral Cerebral Lesions.” *Neuropsychologia* 3 (4): 317–38. https://doi.org/10.1016/0028-3932(65)90005-9.

Mishkin, Mortimer. 1978. “Memory in Monkeys Severely Impaired by Combined but Not by Separate Removal of Amygdala and Hippocampus.” *Nature* 273 (5660): 297–98. https://doi.org/10.1038/273297a0.

Otto, T., and H. Eichenbaum. 1992. “Neuronal Activity in the Hippocampus during Delayed Non-Match to Sample Performance in Rats: Evidence for Hippocampal Processing in Recognition Memory.” *Hippocampus* 2 (3): 323–34. https://doi.org/10.1002/hipo.450020310.

Pachitariu, Marius, Carsen Stringer, Mario Dipoppa, Sylvia Schröder, L. Federico Rossi, Henry Dalgleish, Matteo Carandini, and Kenneth D. Harris. 2016. “Suite2p: Beyond 10,000 Neurons with Standard Two-Photon Microscopy.” Preprint. Neuroscience. https://doi.org/10.1101/061507.

Palombo, Daniela J., Margaret M. Keane, and Mieke Verfaellie. 2015. “The Medial Temporal Lobes Are Critical for Reward-Based Decision Making under Conditions That Promote Episodic Future Thinking: DECISION MAKING IN AMNESIA.” *Hippocampus* 25 (3): 345–53. https://doi.org/10.1002/hipo.22376.

Pastalkova, Eva, Vladimir Itskov, Asohan Amarasingham, and György Buzsáki. 2008. “Internally Generated Cell Assembly Sequences in the Rat Hippocampus.” *Science (New York, N.Y.)* 321 (5894): 1322–27. https://doi.org/10.1126/science.1159775.

Quirk, G. J., R. U. Muller, J. L. Kubie, and J. B. Ranck. 1992. “The Positional Firing Properties of Medial Entorhinal Neurons: Description and Comparison with Hippocampal Place Cells.” *The Journal of Neuroscience: The Official Journal of the Society for Neuroscience* 12 (5): 1945–63. https://doi.org/10.1523/JNEUROSCI.12-05-01945.1992.

Robinson, Nick T. M., James B. Priestley, Jon W. Rueckemann, Aaron D. Garcia, Vittoria A. Smeglin, Francesca A. Marino, and Howard Eichenbaum. 2017. “Medial Entorhinal Cortex Selectively Supports Temporal Coding by Hippocampal Neurons.” *Neuron* 94 (3): 677-688.e6. https://doi.org/10.1016/j.neuron.2017.04.003.

Ross, J. F., L. L. Walsh, and S. P. Grossman. 1973. “Some Behavioral Effects of Entorhinal Cortex Lesions in the Albino Rat.” *Journal of Comparative and Physiological Psychology* 85 (1): 70–81. https://doi.org/10.1037/h0034864.

Sabariego, Marta, Antonia Schönwald, Brittney L. Boublil, David T. Zimmerman, Siavash Ahmadi, Nailea Gonzalez, Christian Leibold, Robert E. Clark, Jill K. Leutgeb, and Stefan Leutgeb. 2019. “Time Cells in the Hippocampus Are Neither Dependent on Medial Entorhinal Cortex Inputs nor Necessary for Spatial Working Memory.” *Neuron* 102 (6): 1235-1248.e5. https://doi.org/10.1016/j.neuron.2019.04.005.

Salz, Daniel M., Zoran Tiganj, Srijesa Khasnabish, Annalyse Kohley, Daniel Sheehan, Marc W. Howard, and Howard Eichenbaum. 2016. “Time Cells in Hippocampal Area CA3.” *The Journal of Neuroscience: The Official Journal of the Society for Neuroscience* 36 (28): 7476–84. https://doi.org/10.1523/JNEUROSCI.0087-16.2016.

Sargolini, Francesca, Marianne Fyhn, Torkel Hafting, Bruce L. McNaughton, Menno P. Witter, May-Britt Moser, and Edvard I. Moser. 2006. "Conjunctive Representation of Position, Direction, and Velocity in Entorhinal Cortex." *Science (New York, N.Y.)* 312 (5774): 758–62. https://doi.org/10.1126/science.1125572.

Schenk, F., F. Inglin, and M. Gyger. 1983. "Activity and Exploratory Behavior after Lesions of the Medial Entorhinal Cortex in the Woodmouse (Apodemus Sylvaticus)." *Behavioral and Neural Biology* 37 (1): 89–107. https://doi.org/10.1016/s0163-1047(83)91103-2.

Scoville, W. B., and B. Milner. 1957. "Loss of Recent Memory after Bilateral Hippocampal Lesions." *Journal of Neurology, Neurosurgery, and Psychiatry* 20 (1): 11–21. https://doi.org/10.1136/jnnp.20.1.11.

Skaggs, W, McNaughton B. 1992. "An Information-Theoretic Approach to Deciphering the Hippocampal Code." *Advances in Neural Information Processing Systems* 5.

Squire, L. R., and S. Zola-Morgan. 1991. "The Medial Temporal Lobe Memory System." *Science (New York, N.Y.)* 253 (5026): 1380–86. https://doi.org/10.1126/science.1896849.

Steffenach, Hill-Aina, Menno Witter, May-Britt Moser, and Edvard I. Moser. 2005. "Spatial Memory in the Rat Requires the Dorsolateral Band of the Entorhinal Cortex." *Neuron* 45 (2): 301–13. https://doi.org/10.1016/j.neuron.2004.12.044.

Stensola, Hanne, Tor Stensola, Trygve Solstad, Kristian Frøland, May-Britt Moser, and Edvard I. Moser. 2012. "The Entorhinal Grid Map Is Discretized." *Nature* 492 (7427): 72–78. https://doi.org/10.1038/nature11649.

Toda, Koji, Nicholas A. Lusk, Glenn D. R. Watson, Namsoo Kim, Dongye Lu, Haofang E. Li, Warren H. Meck, and Henry H. Yin. 2017. "Nigrotectal Stimulation Stops Interval Timing in Mice." *Current Biology: CB* 27 (24): 3763-3770.e3. https://doi.org/10.1016/j.cub.2017.11.003.

Tsao, Albert, Jørgen Sugar, Li Lu, Cheng Wang, James J. Knierim, May-Britt Moser, and Edvard I. Moser. 2018. "Integrating Time from Experience in the Lateral Entorhinal Cortex." *Nature* 561 (7721): 57–62. https://doi.org/10.1038/s41586-018-0459-6.

Tulving, Endel. 1984. "Précis of Elements of Episodic Memory." *Behavioral and Brain Sciences* 7 (2): 223–38. https://doi.org/10.1017/S0140525X0004440X.

Verhagen, Justus V., Daniel W. Wesson, Theoden I. Netoff, John A. White, and Matt Wachowiak. 2007. "Sniffing Controls an Adaptive Filter of Sensory Input to the Olfactory Bulb." *Nature Neuroscience* 10 (5): 631–39. https://doi.org/10.1038/nn1892.

Vo, Annette, Nina S. Tabrizi, Thomas Hunt, Kayla Cayanan, Saee Chitale, Lucy G. Anderson, Sarah Tenney, André O. White, Marta Sabariego, and Jena B. Hales. 2021. "Medial Entorhinal Cortex Lesions Produce Delay-Dependent Disruptions in Memory for Elapsed Time." *Neurobiology of Learning and Memory* 185 (November): 107507. https://doi.org/10.1016/j.nlm.2021.107507.

Witter, Menno P. 2003. "Organization of Cortico-Hippocampal Networks in Rats Related to Learning and Memory." *International Congress Series* 1250 (October): 131–45. https://doi.org/10.1016/S0531-5131(03)01014-8.

Yartsev, Michael M., Menno P. Witter, and Nachum Ulanovsky. 2011. "Grid Cells without Theta Oscillations in the Entorhinal Cortex of Bats." *Nature* 479 (7371): 103–7. https://doi.org/10.1038/nature10583.

Yoon, Kijung, Michael A. Buice, Caswell Barry, Robin Hayman, Neil Burgess, and Ila R. Fiete. 2013. "Specific Evidence of Low-Dimensional Continuous Attractor Dynamics in Grid Cells." *Nature Neuroscience* 16 (8): 1077–84. https://doi.org/10.1038/nn.3450.

Ziv, Yaniv, Laurie D. Burns, Eric D. Cocker, Elizabeth O. Hamel, Kunal K. Ghosh, Lacey J. Kitch, Abbas El Gamal, and Mark J. Schnitzer. 2013. "Long-Term Dynamics of CA1 Hippocampal Place Codes." *Nature Neuroscience* 16 (3): 264–66. https://doi.org/10.1038/nn.3329.

Zola-Morgan, S., L. R. Squire, and D. G. Amaral. 1986. "Human Amnesia and the Medial Temporal Region: Enduring Memory Impairment Following a Bilateral Lesion Limited to Field CA1 of the Hippocampus." *The Journal of Neuroscience: The Official Journal of the Society for Neuroscience* 6 (10): 2950–67. https://doi.org/10.1523/JNEUROSCI.06-10-02950.1986.

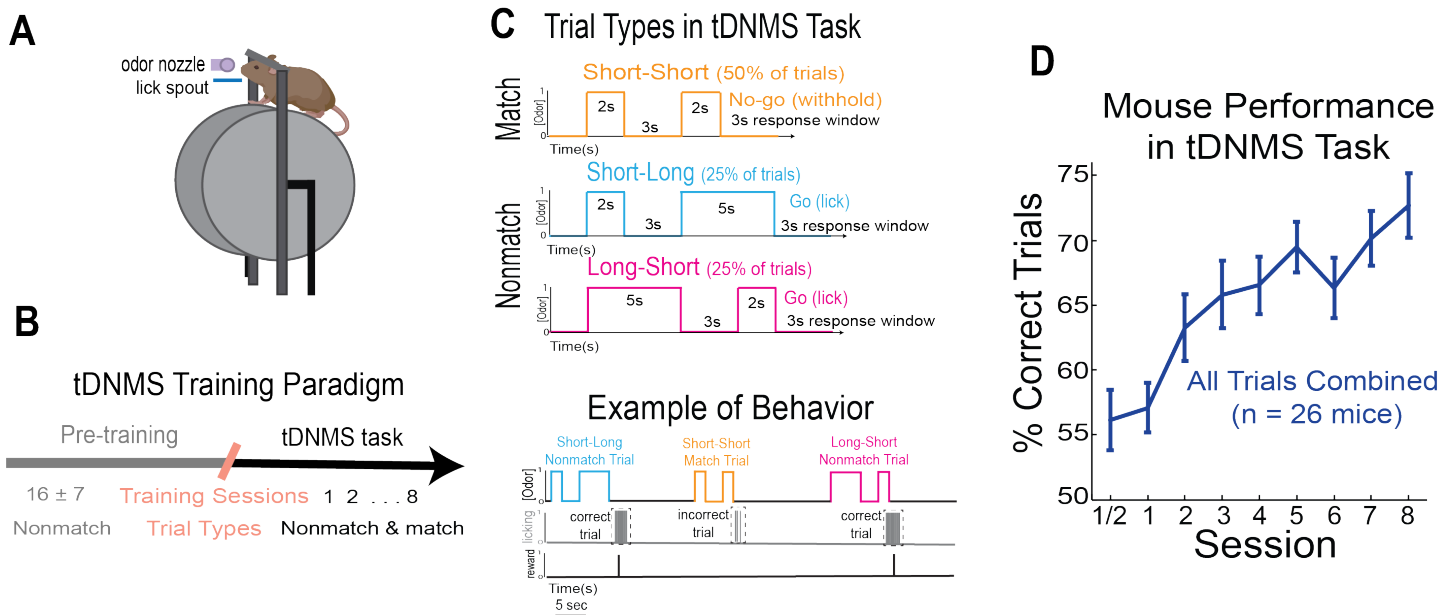

Figure 1. Mice learn a novel tDNMS task. A. Simplified experimental set-up. **B.** Overview of training paradigm. Mice are first pre-trained to lick at the offset of nonmatched trials to trigger reward delivery. Upon reaching criteria after an average of 16 sessions, mice began 8 training sessions in the tDNMS task, where matched trials are introduced. Number of session shown as mean +/- standard deviation. **C.** Trial types and example behavior. The tDNMS task consists of 3 types of trials defined by stimulus durations: short-short, short-long and long-short. To perform the task correctly, mice must lick in the response window following non-matched trials and withhold licking in matched trials. **D.** Percent correct for all trial types for each session, averaged across all mice (n = 26 mice).

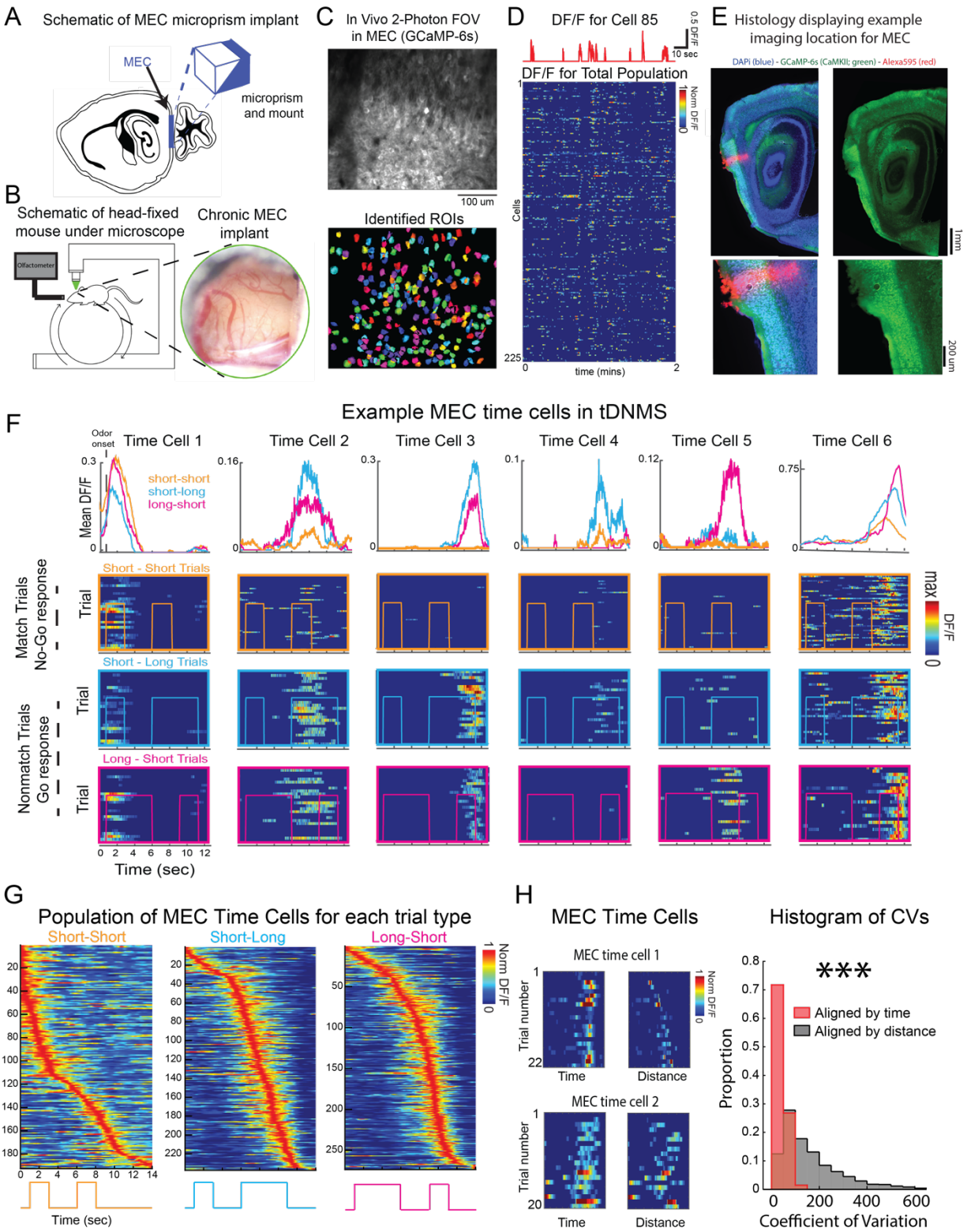

Figure 2. MEC time cells exhibit context-dependent sequential neural activity. A. Optical approach for imaging in MEC. **B.** Left, mouse positioned on the cylindrical treadmill and underneath the two-photon microscope. Olfactometer delivers odor near mouse snout. Right, image of MEC prep following chronic implant. **C.** Average image of example FOV labelled with GCaMP-6S (top) and ROIs from this FOV (below). **D.** Example dF/F time series for individual neuron (top) and all ROIs from panel C. **E.** Representative histology. Red pin mark indicates relative location of imaging field. **F.** Example individual MEC time cells. MEC time cells 1,2 and 6 are active across all trial types (i.e. context independent). MEC time cells 3-5 are active on specific trial types (i.e. context-dependent). **G.** All MEC time cells sorted for each trial type. **H.** Left, example time cells plotted as a function of elapsed time and distance travelled from trial onset. Right, distribution of coefficient of variation for all MEC time cells, measured as a function of elapsed time and distance travelled from trial onset.

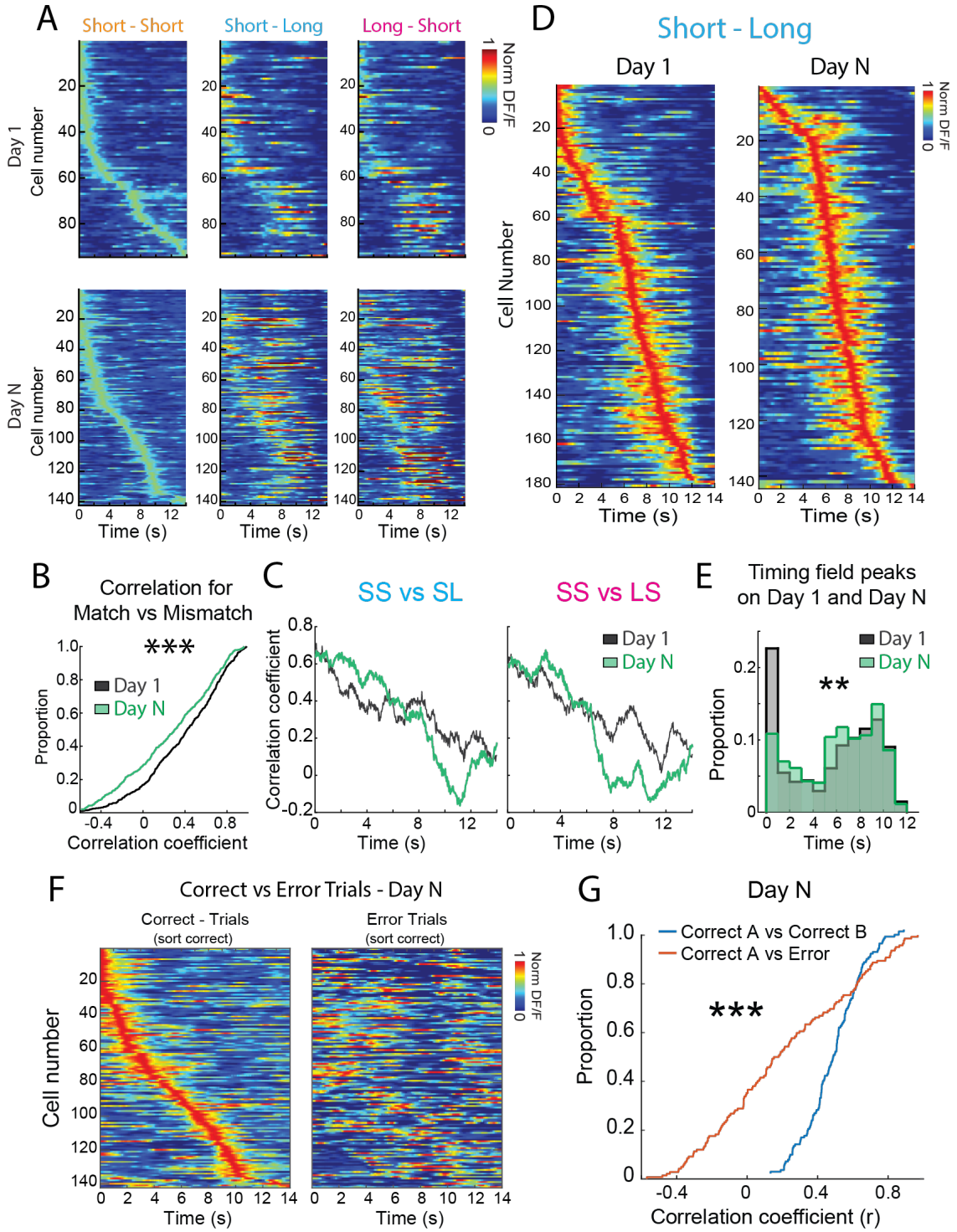

Figure 3. Context-dependent MEC time cell population dynamics support learning of flexible interval timing behavior. A. Top, population of MEC time cells (significant for short-short trials; sorted by short-short trials) for short-short trials (left), short-long trials (middle) and long-short trials (right) on day 1. Bottom, same as above except for day N sessions. **B.** Cumulative distribution for Pearson's Correlation Coefficient computed for each MEC time cell's activity across trial types for day 1 (black) and day N (green). **C.** Left, Pearson's Correlation, plotted as a function of time during trial, for time cell activity for short-short trials versus short-long on day 1 (black) and day N (green). Right, same as left, expect for short-short versus long-short time cell activity. D. Sorted sequence of MEC time cells in short-long trials on day 1 (left) and day N (right). **E.** Histogram for peaks of time fields for all MEC time cells on day 1 (black) and day N (green), for all 3 trial types. **F.** MEC time cells on short-short correct trials (left) and on short-short error trials on day N of training in tDNMS task. **G.** Cumulative distribution of Pearson's Correlation Coefficient computed for MEC time cells on correct (blue) versus error trials (red) (see methods).

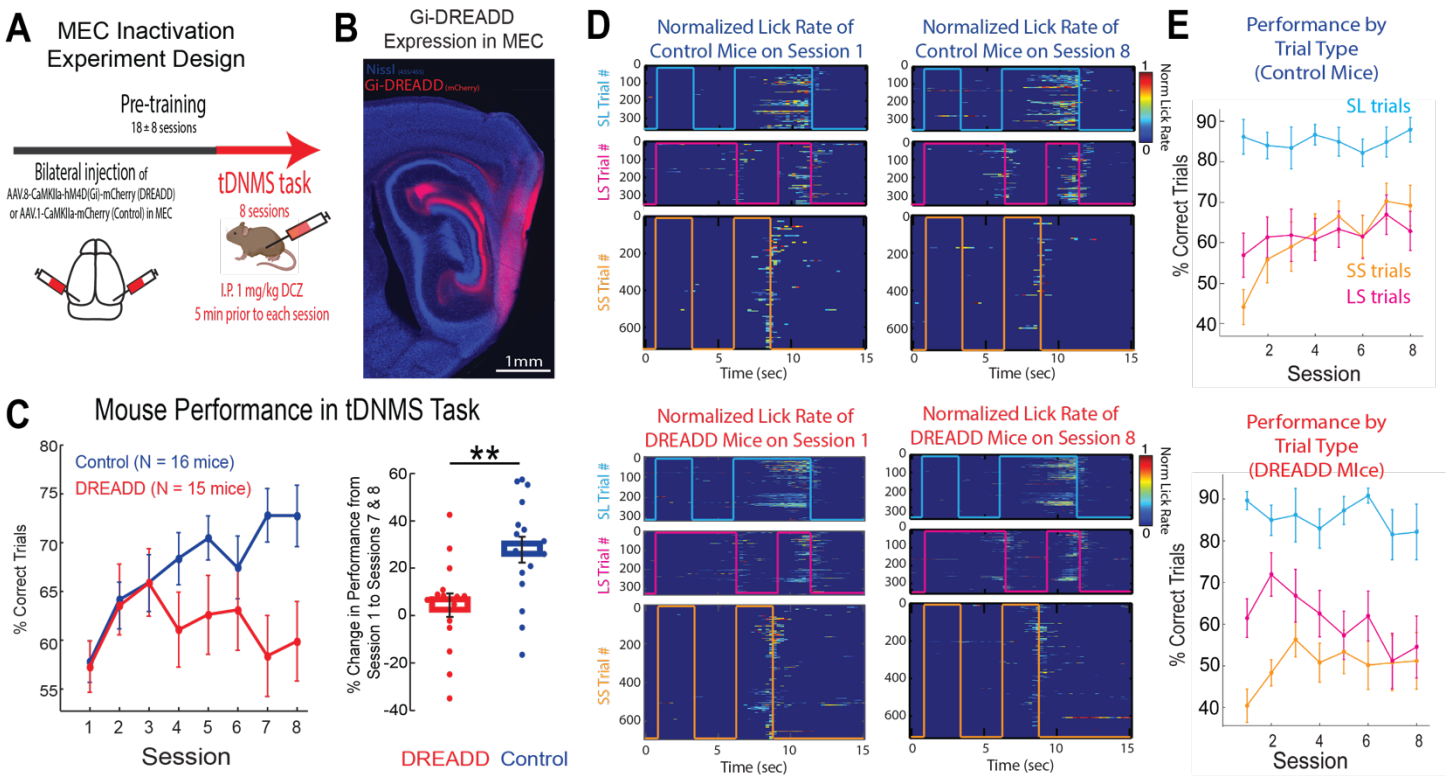

Figure 4. MEC is necessary to learn the tDNMS task. A. Experimental paradigm. Mice received bilateral injections of either an inhibitory DREADD (n=15) or control virus (n=16). Mice began pre-training with only nonmatch trials and learned to lick at the offset of the second odor stimuli. Following pre-training mice began the tDNMS task. DREADD agonist DCZ (1mg/kg) was administered via I.P. 5 minutes prior to each of the 8 tDNMS sessions. **B.** Sagittal section depicting hM4D(Gi)-mCherry expression in MEC with blue NeuroTrace staining. **C.** Left, performance on the tDNMS task differs for control (blue) and DREADD (red) (Repeated measures ANOVA Group Type x Time $F(7,7) = 2.69$, $p<0.05$). Right, percent change in correct response from day 1 to average of days 7 and 8 ($p<0.01$, unpaired Student's t-test). **D.** Top, Licking behavior during tDNMS task for control mice on session 1 (left) and session 8 (right) for all 3 trial types. Bottom, Licking behavior during tDNMS task for DREADD mice on session 1 (left) and session 8 (right) for all 3 trial types. **E.** Average correct response for control (top) and DREADD mice (bottom) for all three trial types. Control mice show an improvement in match trials (Repeated measures ANOVA Group Type x Time $F(7,15) = 5.93$, $p<0.001$) compared to DREADD mice (Repeated measures ANOVA Group Type x Time $F(7,14) = 5.93$, $p<0.15$). Bars indicate mean +/- SEM.

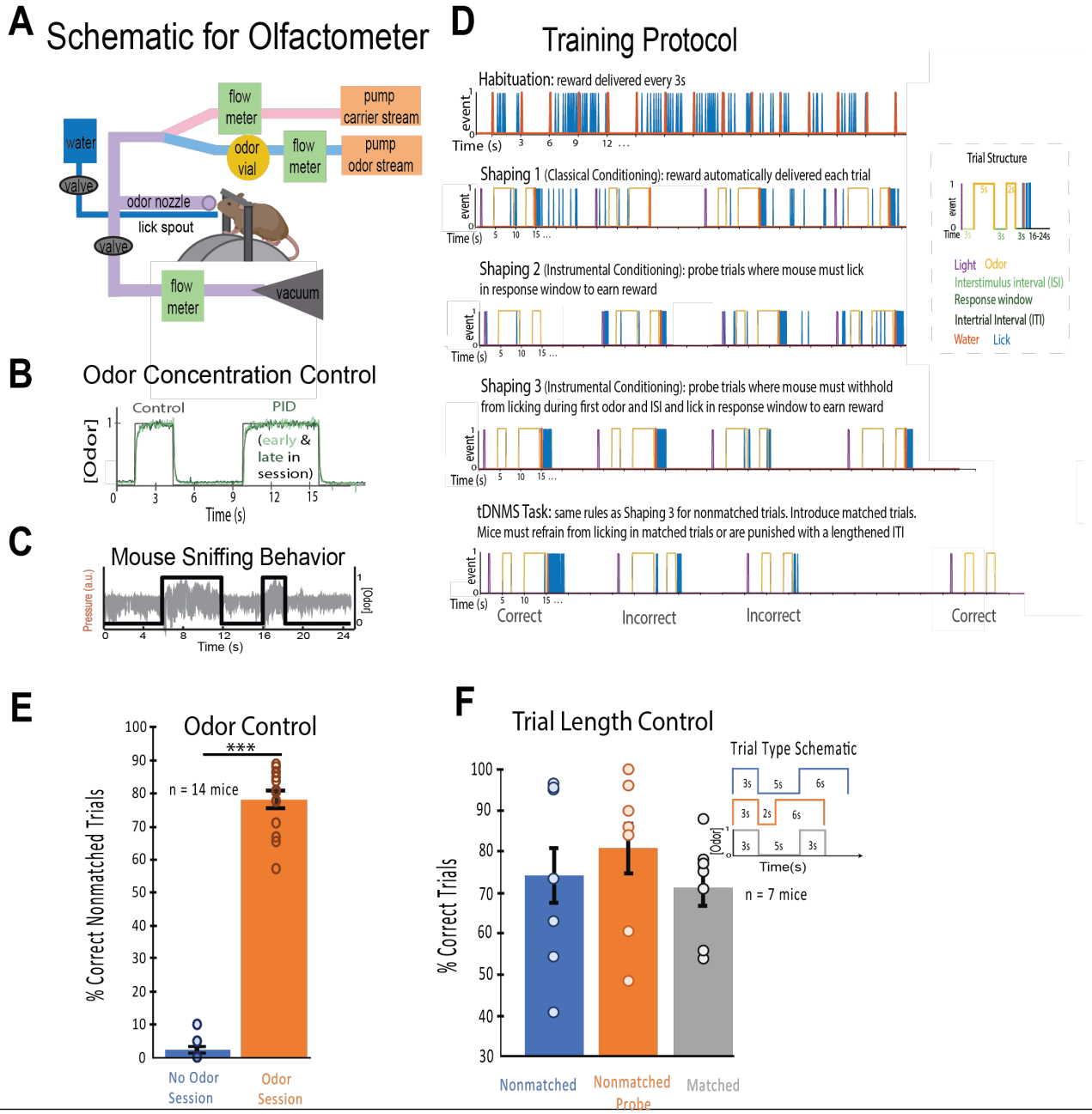

Figure S1. tDNMS Set-Up and Control. A. Experimental set-up. Odorized air is directed either to the mouse or to a vacuum. A lick spout, connected to a capacitance sensor, delivers water and is used to monitor mouse licking. **B.** Odor concentration control. Odor concentration was measured using a photoionization detector (PID). Odor concentration can be controlled with high temporal specificity at a constant concentration over 45 minutes, as shown by PID measurements (green) relative to control signals (black). **C.** Sniffing behavior measured by a flow meter during a sample trial. **D.** Training protocol. Mice undergo three phases of pretraining (see methods). **E.** Odor control. After completing tDNMS training, mice were tested with no odorant (mineral oil only). Mice failed to solve the nonmatch trials in the absence of odor but performed well in a prior session in which odor was used (2.25 +/- 1.01 % correct responses for no odor condition compared to 78.08 +/- 2.58% correct with odor, $p<0.001$ Student's Paired T-Test; n=14 mice). Bars represent mean +/- SEM. **F.** Trial length control session. The ISI was manipulated on a random subset of nonmatched trials ("probe trials") such that overall trial duration was identical to the matched trial duration. If mice use total trial duration to solve the task, rather than comparing individual stimuli durations, then they should incorrectly withhold licking on probe trials. Instead, there was no significant difference between nonmatch (74.14 +/- 6.71%) and probe trial performance (80.71 +/- 6.02%) ($p=0.19$ Student's paired T-test; n=7 mice). Bars indicate mean +/- SEM.

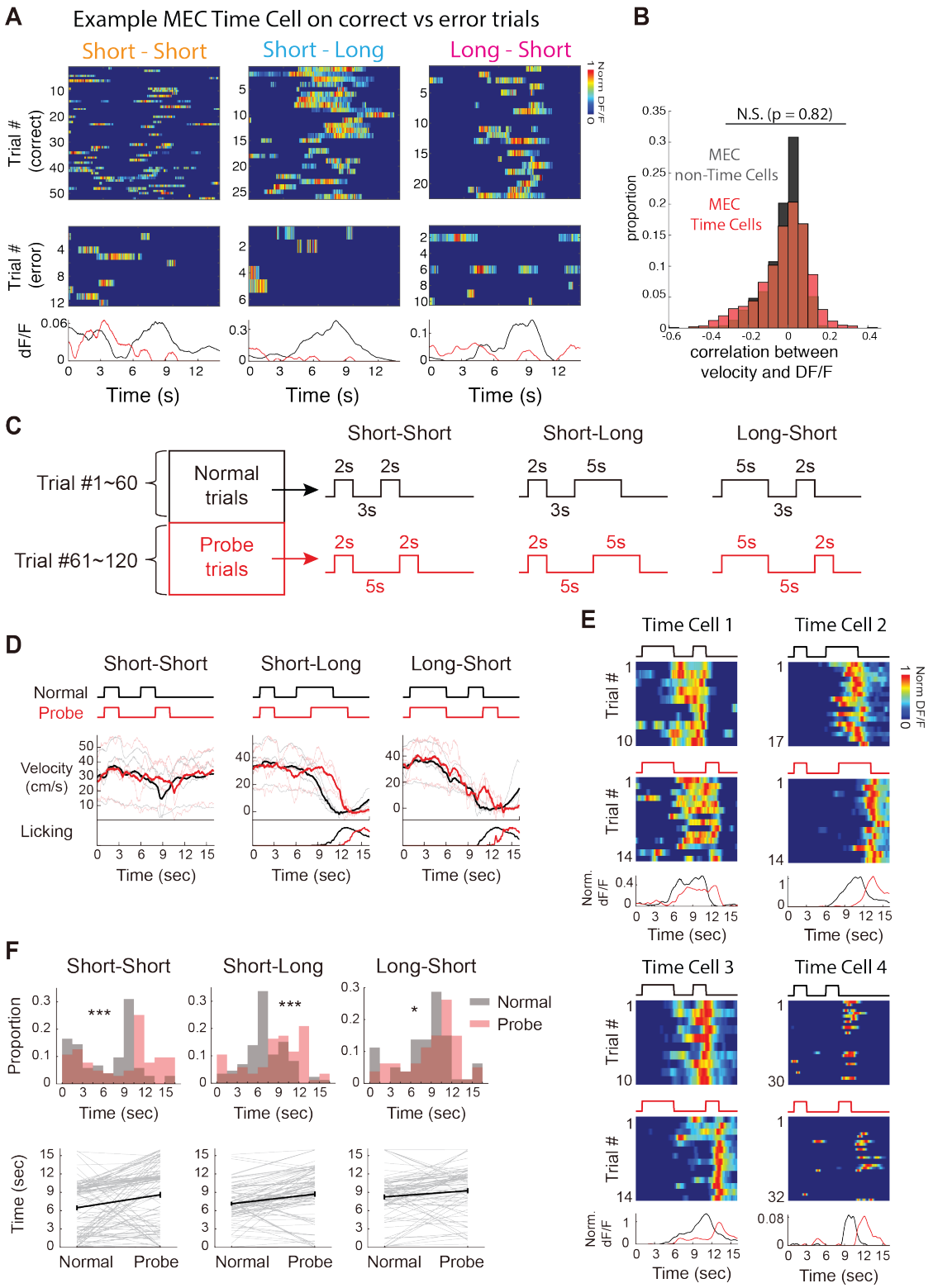

Figure S2. MEC time cells on ISI probe trials. A. Example MEC time cell activity on short-short, short-long and long-short correct (top) and error (bottom) trials. **B.** Histogram of Pearson's Correlation Coefficients for DF/F versus velocity for MEC time cells (red) and non-Time Cells (black). **C.** Schematic for probe trials. **D.** Mean velocity and licking on short-short, short-long and long-short conditions during control (black) and probe trials (red). **E.** four example MEC time cells during control (black) and probe (red) trials. **F.** Time of peak response across the population of MEC time cells on short-short, short-long and long-short conditions during control (black) and probe trials (red).

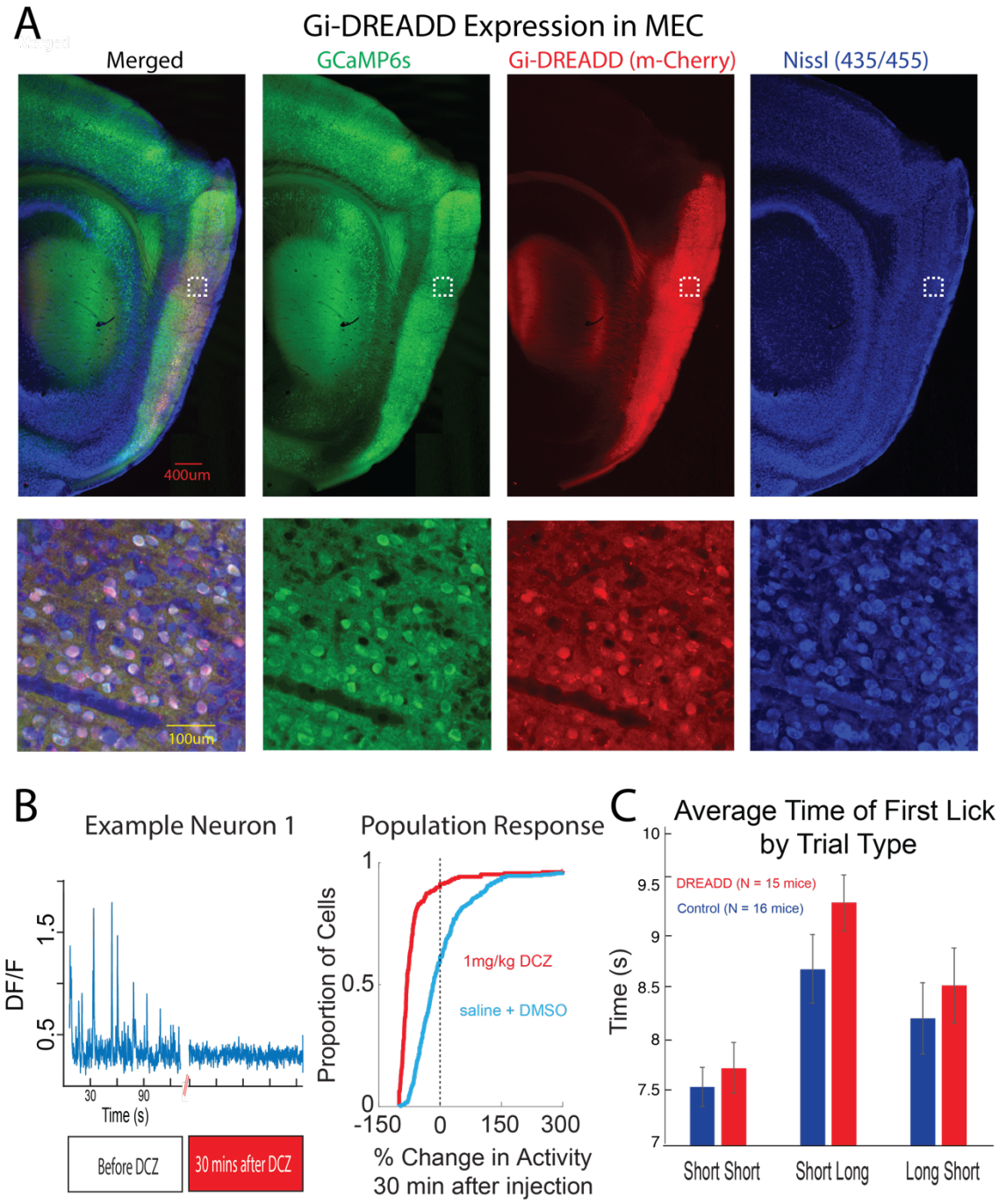

Figure S3. MEC DREADD inactivation. A. Histology showing co-expression of GCaMP6s and hM4D(Gi)-m-Cherry in MEC. **B** Simultaneous in vivo 2-photon GCaMP6s imaging and hM4Di inactivation in MEC. Activation of inhibitory DREADD receptor by 1 mg/kg IP injection of DCZ reduces average number of Ca2+ transients in MEC neurons by 80% at 30 minutes post injection compared to before DCZ injection. In both the control (blue) and DCZ (red) conditions, GCaMP activity was monitored in populations of neurons over 5 minute periods and the change in activity was measured within for each cell (n=302 neurons in 2 mice; P<0.01 Kolmogorov-Smirnov test). **C.** Average time of first lick relative to odor onset. During matched short-short trials, control (n=16) mice first licked at 7.58 +/- 0.19s compared to 7.76 +/- 0.25s for DREADD mice (n=15) (p=0.56 Student's unpaired T-test). During nonmatched short-long trials, control (n=16) mice first licked at 8.73 +/- 0.33s compared to 9.37 +/- 0.28s for DREADD mice (n=15) (p=0.14 Student's unpaired T-test). During nonmatched long-short trials, control (n=16) mice first licked at 8.24 +/- 0.35s compared to 8.56 +/- 0.36s for DREADD mice (n=15) (p=0.52 Student's unpaired T-test). Data indicate mean +/- SEM

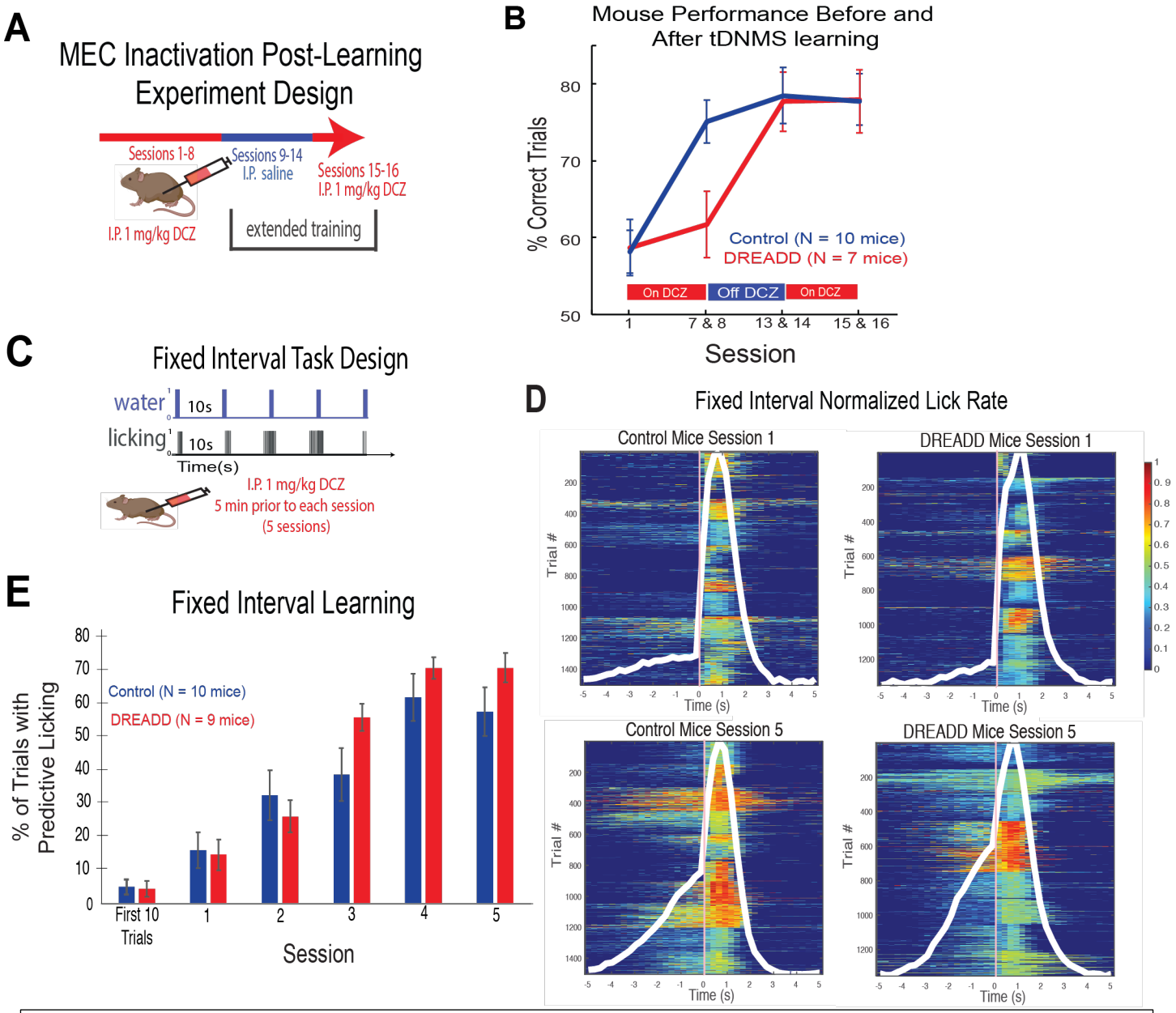

Figure S4. MEC is not required for all interval timing behavior. A. Schematic for inhibiting MEC after learning in the tDNMS task. Following experiments testing the role of MEC during learning (Figure 4), a subset of mice underwent extended training to determine whether MEC activity is necessary for ongoing performance in the tDNMS task. **B.** Though MEC inhibition completely abolished normal performance in the tDNMS task during learning (Sessions 1-8), DREADD mice learned the task in the absence of MEC inhibition (Sessions 9-14). Following learning in sessions 9-14, subsequent administration of DCZ to inactivate MEC did not affect performance in Sessions 15 and 16 (-0.38 +/- 4.01% change in correct response from sessions 13&14 compared to sessions 15&16 in Control mice (n=10) versus 2.19 +/- 7.30% change in correct response from sessions 13&14 compared to sessions 15&16 in DREADD mice (n=7); p=0.74 Student's unpaired T-test). **C.** Fixed interval task schematic. MEC DREADD and Control mice were trained on a Fixed Interval task (Toda et al. 2017). A droplet of water (4-6ul) was delivered every 10s to head-fixed mice. Licking was measured; time-locked predictive licking indicated learning of timing of water delivery. **D.** Licking behavior of DREADD (n=9) and Control (n=10) mice on sessions 1 and 5 of the Fixed Interval Task. Licking was normalized to the maximum lick frequency with each session for each mouse. All trials for all mice are shown, and water delivery occurs at 0s, indicated by line. Average lick response for each session is shown (white). **E.** Fixed interval learning. Predictive licking is defined as an increase in lick rate, measured over 5 seconds preceding the upcoming reward delivery. Predictive licking is not statistically significantly different for Control compared to DREADD mice (Repeated Measures ANOVA Group x Time $F_{4,4} = 1.98$, $p=0.11$). Data represent mean +/- SEM.

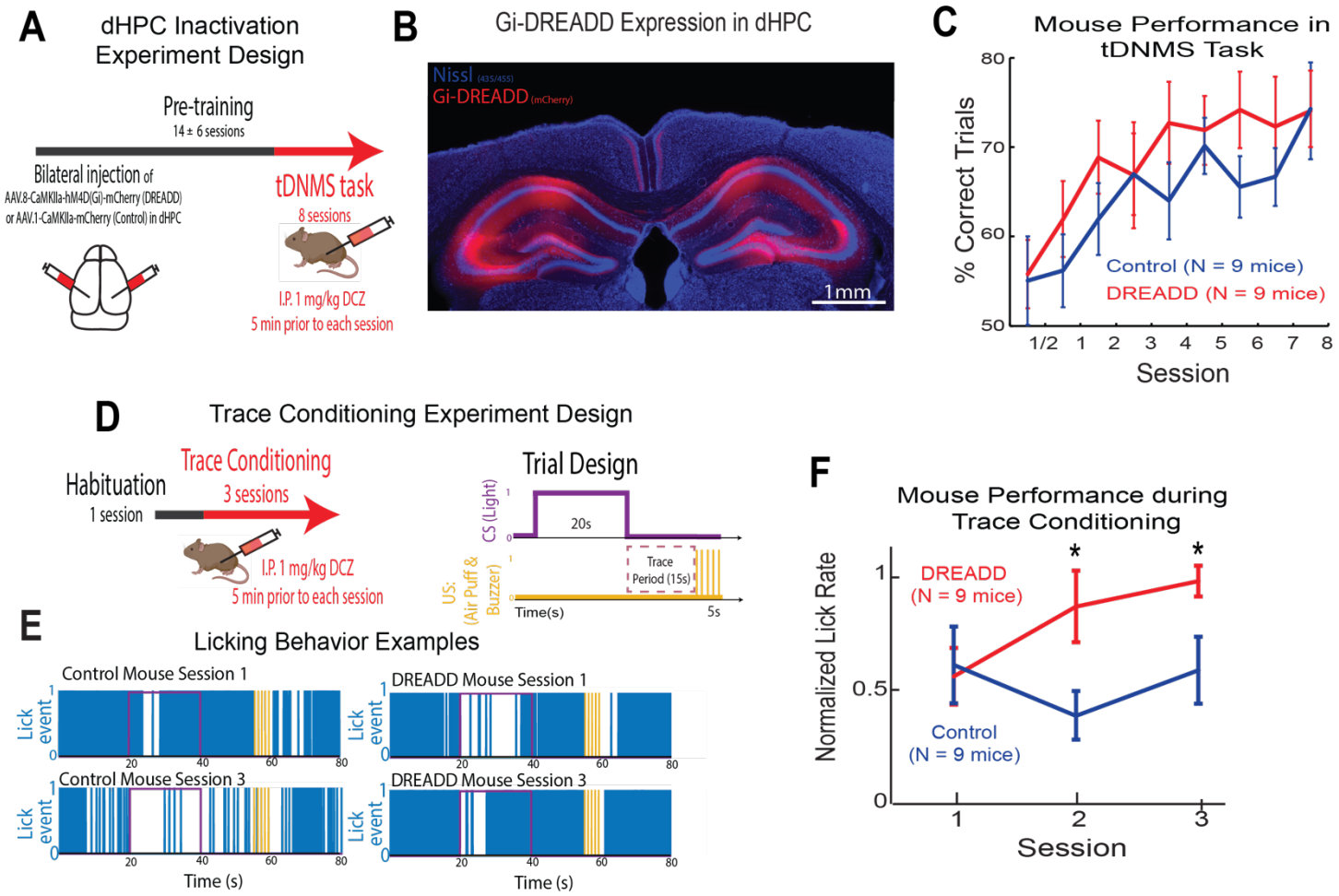

Figure S5. Dorsal Hippocampus (dHPC) is not necessary to learn the tDNMS task. A. Schematic for dHPC inactivation during learning. **B.** Coronal section showing hM4D(Gi)-mCherry (red) expression in dHPC with fluorescent Nissl staining (blue). **C.** tDNMS learning. Control and DREADD mice display learning in the tDNMS task over 8 session of 1 mg/kg DCZ injections (same protocol as for MEC inactivation in Figure 4). Data represent mean +/- SEM. (Repeated Measures ANOVA Group x Time $F_{7,7} = 0.72$, $p = 0.65$). **D.** Trace conditioning paradigm. Control and DREADD mice were trained using a conditioning task like described in Ahmed et al. 2020. Briefly, mice were trained to lick to earn water rewards (<2ul). Following this habituation phase, mice were then trained on a trace conditioning paradigm in which a 20s conditioned stimulus (CS) was presented, followed by a 15 second trace period and finally an unconditioned stimulus (US: mild air puff). Mice are expected to withhold licking during the CS if they have learned to associate the CS with US. **E.** Example licking behavior during first trial of Session 1(top) and Session 3 (bottom) for control (left) and DREADD mouse (right). Licking is shown in blue. **F.** Trace conditioning performance on the first trial of each of the 3 sessions. Licking was measured during the CS and was normalized to baseline licking in the 20s preceding the CS. During session 3, control mice (n=9) reduced licking 40.76 +/- 14.86% compared to DREADD (n=9) mice that showed a 1.17 +/- 6.85 % change; $p<0.05$ Student's unpaired T-test. Note, the same group of 9 control and 9 DREADD mice were used for tDNMS and trace conditioning experiments.